Materials Sciences and Applications, **2013, 4, 77-102**
http://dx.doi.org/10.4236/msa.2013.41010 Published Online January 2013 (http://www.scirp.org/journal/msa)

FE Modeling and Analysis of Isotropic and Orthotropic Beams Using First Order Shear Deformation Theory

M. Adnan Elshafei*

Aeronautical Department, Military Technical Collage, Cairo, Egypt.
Email: *maelshafei@yahoo.com

Received October 26th, 2012; revised November 12th, 2012; accepted December 11th, 2012

ABSTRACT

In the present work, a finite element model is developed to analyze the response of isotropic and orthotropic beams, a common structural element for aeronautics and astronautic applications. The assumed field displacements equations of the beams are represented by a first order shear deformation theory, the Timoshenko beam theory. The equations of motion of the beams are derived using Hamilton's principle. The shear correction factor is used to improve the obtained results. A MATLAB code is constructed to compute the natural frequencies and the static deformations for both types of beams with different boundary conditions. Numerical calculations are carried out to clarify the effects of the thickness-to-length ratio on both the Eigen values and the deflections of the beams due to the applied mechanical load. The obtained results of the proposed model are compared to the available results of other investigators, good agreement is generally obtained.

Keywords: Finite Element Method; Timoshenko Beam Theory; Composite Materials Mechanics; Static and Dynamic Analysis of Beams

1. Introduction

The current trend of aeronautics and astronautic design is to use large, complex, and light-weight structures elements. These structures are commonly having low-frequency fundamental vibration modes in addition to fabricate by graphite-epoxy to satisfy the requirements of minimum weight and low thermal distortion. Because of that several researchers are interested to solve the beam structures by different theories.

Yuan and Miller [1], proposed finite element model for laminated composite beams with separate rotational degrees of freedom for each lamina. The shear deformation is included in the model but the interfacial slip or delamination is not included. Their element can be used even for short beams with many laminas. The model results was compared with those of other theoretical and experimental investigations and found reasonable.

Chandrashekhara and Bangera [2], developed finite element model based on a higher-order deformation theory with Poisson's effect is incorporated. They concluded the following: 1) The shear deformations decrease the natural frequencies of the beam; 2) The natural frequencies increase with the increase of the number of beam layers; 3) The clamped-free boundary condition exhibits the lowest frequencies; 4) The increase of fiber orientation angle decreases the natural frequency; and 5) the natural frequency decreases by increasing the material anisotropy.

Friedman and Kosmatka [3], developed two-node Timoshenko beam element using Hamilton's principal. The resulting stiffness matrix of their model was exactly integrated and it was free of "shear-locking", and it was in agreement with the exact Timoshenko beam stiffness matrix. Their element was exactly predicting the displacement of short beam subjected to distributed loads and also predicted the natural frequencies.

Lidstrom [4], derived an equilibrium formulation of 3D beam element using the energy derivatives. His formulation contains the coupling terms between translation and twist, also between translational bending and elongation. A three node element was introduced in such model. Also condensed two node version of the element has been analyzed. He found that two-node system was less numerically stable than the proposed three-node system.

Bhate *et al.* [5], proposed a refined flexural theory for composite beam based on the potential energy concept. The warping effect is included in their formulation; however the shear correction coefficient was eliminated. They found that their theory is established for short composite beams where cross-sectional warping is predominant.

*Corresponding author.

Copyright © 2013 SciRes.

Nabi and Ganesan [6], studied the free vibration characteristics of composite beams using finite element model based on a first-order deformation theory including bi-axial bending as well as torsion. They studied the effect of shear-deformation, beam geometry, and boundary conditions on the natural frequencies. They concluded that the natural frequencies are 1) Decrease with the increase of fiber orientation angle; 2) Increase with the increase of the beam length to height ratio for all fiber orientation angles; 3) Also have the lowest value in case of clamped-free boundary conditions

Armanios and Badir [7], evaluated analytically the effect of elastic coupling mechanisms on vibration behaveior of thin-walled composite beams. Good agreement was found between their results and those developed by Giavotto *et al*. (1983) [8], and Hagodes *et al*. (1991) [9], based on finite element technique, and the experimental measurements obtained by Chandra and Chopra [10].

Rao and Ganesan [11], investigated a Harmonic response of tapered composite beams using finite element model based on a higher order shear deformation theory. The uniaxial bending and the Poisson ratio effect were considered and the interlaminar shear stresses were neglected. The effect of in-plane inertia and rotary inertia were also considered in their formulation of the mass matrix. A parametric study is done of the influence of anisotropy, taper profile and taper parameter. They found that the transversal displacement is higher than that of a uniform beam. For the taper parameter effect, they deduced that the frequency decreases with increase thickness variations and vise-verse.

Khdeir and Reddy [12], presented an exact solution of the governing equations for the bending of laminated beams. They used the classical, the first-order, the second-order, and the third-order beam theories in their analysis. They studied the effect of shear deformation, number of layers, and the orthotropic ratio on the static response of composite beams. They found large differences between the predicted deflections by the classical beam theory and the higher order beam theories, especially when the ratio of beam length to its height was low due to the shear deformation effects.

Yildirim *et al*. [13], studied the in-plane free vibration of laminated beams based on the transfer matrix method. They considered rotary inertia, shear, and extensional deformation effects on the Timoshenko's beam analysis. Good predictions are obtained and compared to other reporters for different modes of the natural frequencies.

Chakraborty *et al*. [14], proposed a refined looking free first order shear deformable finite element model to solve free vibration and wave propagation problems in laminated composite beam. They developed element, that its shape functions is dependent not only on the length of the element, but also on its material and cross-sectional properties. The developed stiffness matrix is exact while the mass distribution is approximate. Rotary inertia and effect of geometric and material asymmetry is taken into account. They named the model as refined first order deformable element (RFSDE).

Eisenberger [15], proposed exact stiffness coefficients for isotropic beam using a simple higher order theory, which include cubic variation of the axial displacements over the cross-section of the beam. Their model had three degrees of freedom at each node, one transverse displacement and two rotations. They compared their model results with Bernoulli-Euler and Timoshenko beam models and found acceptable.

Lee and Schultz [16], studied the free vibration of Timoshenko beams and axi-symmetric Mindlin plates. The analysis was based on the Chebyshev pseudospectral method, which has been widely used in the solution of fluid mechanics problems. Different boundary conditions of Timoshenko beams were treated, and numerical results were presented for different thickness-to-length ratios.

Subramanian [17], proposed free vibration analysis of composite beams using Finite elements based on two higher order shear deformation theories. The difference between the two theories is that the first theory assumed a non-parabolic variation of transverse shear stress across the thickness of the beams whereas the second theory assumed parabolic variation. The comparison study showed that natural frequencies predict by his model were better than those obtained by other theories and the considered finite elements.

Simsek and Kocaturk [18], studied the free vibration of isotropic beams based on the third-order shear deformation theory. The boundary conditions are satisfied using Lagrange multipliers which reduced the solution of a system of algebraic equations. A trial functions for the deflections and rotations of the cross-section of the beam are expressed in polynomial form. Their results are compared with the previous results based on CBT and FSDT.

Jun *et al*. [19], proposed dynamic finite element model for beams based of first-order shear deformation theory. They introduced the influences of Poisson effect, couplings among extensional, bending and torsion deformations, shear deformation and rotary inertia in their formulation. Their obtained results are compared to those previously published and founded in good accuracy.

Lee and Janga [20], presented spectral element model for axially loaded bending-torsion coupled composite beam based on the first-order shear deformation theory, Timoshenko beam model. They found that the use of frequency-dependent spectral element matrix *i.e.* exact dynamic stiffness matrix, provide extremely accurate

Copyright © 2013 SciRes.

solutions, while reducing the total number of degrees-of-freedom to resolve the computational and cost problems.

Nguyen *et al*. [21], presented full closed-form solution of the governing equations of two-layer composite beam. Timoshenko's kinematics assumptions are considered for both layers and the shear connection is modeled through a continuous relationship between the interface shear flow and the corresponding slip. They derived the "exact" stiffness matrix using the direct stiffness method. They found that the effect of shear flexibility on the deflection is generally more important for composite beams characterized by substantial shear interaction.

Lina and Zhang [22], proposed a two-node element with only two degrees of freedom per node for finite element analyses of isotropic and composite beams. Their model was based on Timoshenko theory. They concluded that their proposed model is accurate and computationally efficient for analysis of isotropic and composite beams.

Kennedya *et al*. [23], presented Timoshenko beam theory for layered orthotropic beams. The proposed theory yields Cowper's shear correction for single isotropic layer, while for multiple layers new expressions for the shear correction factor are obtained. The body-force correction was shown to account for the difference between Cowper's shear correction and the factor originally proposed by Timoshenko. Numerical comparisons between the theory and finite-elements results showed good agreement.

In the present work, a finite element model is proposed, based on first order shear deformation theory, Timoshenko beam theory, with a shear correction factor, to predict the static responses and dynamic characteristics of advanced isotropic and orthotropic beams for different boundary conditions and different length to thickness ratio due to different applied loads. The structure outline of the present work can be drawn for both isotropic and orthotropic beams as follows:

1) Theoretical formulation using the Timoshenko theory.

2) Finite element formulation to obtain the structure equation of motion.

3) The model validation and parametric studies which contain the items:

a) Model convergence for both deflection and eigenvalues.

b) Static deformation of the beam.

c) Dynamic characteristics of the beam.

d) Model predictions analysis and conclusions.

2. Theoretical Formulation

The displacements field equations of the beam are assumed as follows [12]:

$$u(x,z)=u_o(x)-z\left[c_o\frac{\mathrm{d}w}{\mathrm{d}x}+c_1\phi(x)\right]+c_2z^2\psi(x)+c_3\left(\frac{z}{h}\right)^3\left[\phi(x)+\frac{\mathrm{d}w}{\mathrm{d}x}\right] \tag{1a}$$

$$v(x,z)=0 \tag{1b}$$

$$w(x,z)=w_o(x) \tag{1c}$$

where u, v and w are the displacements field equations along the coordinates x, y and z, respectively, u_0 and w_0 denote the displacements of a point $(x,y,0)$ at the mid plane, $\phi(x)$ $\phi(x)$ and $\psi(x)$ are the rotation angles of the cross-section as shown in **Figure 1**.

By selecting the constant values of Equation (1) a as: $c_0=0,\ c_1=1,\ c_2=0,\ c_3=0$, the displacements field equations for first-order theory (FOBT) at any point through the thickness can be expressed as [24]:

$$\begin{aligned}u(x,z)&=u_o(x)-z\phi(x)\\ v(x,z)&=0\\ w(x,z)&=w_o(x)\end{aligned} \tag{2}$$

The strain-displacement relationships are obtained by differentiating the assumed displacement field equations, Equation (2), as follows:

$$\varepsilon_{xx}(x,y,z)\equiv\frac{\partial u(x,y,z)}{\partial x}=\frac{\partial u_o(x,z)}{\partial x}-z\frac{\partial\phi_o(x,z)}{\partial x}=\varepsilon_{xx}^{\circ}+z\kappa_{xx}^{\circ} \tag{3a}$$

$$\gamma_{xz}(x,y,z)=\frac{\partial u(x,y,z)}{\partial x}+\frac{\partial w(x,y,z)}{\partial x}=-\phi_x+\frac{\mathrm{d}w_o}{\mathrm{d}x}=\gamma_{xz}^{\circ} \tag{3b}$$

The strains at any point through the thickness of the beam can be written in matrix form as:

$$\begin{Bmatrix}\varepsilon_{xx}\\ \gamma_{xz}\end{Bmatrix}=\begin{Bmatrix}\varepsilon_{xx}^{\circ}\\ \gamma_{xz}^{\circ}\end{Bmatrix}+z\begin{Bmatrix}\kappa_{xx}^{\circ}\\ \kappa_{xz}^{\circ}\end{Bmatrix} \tag{4}$$

The components ε_{xx}° γ_{xz}° and κ_{xx}° are the reference surface extensional strain in the x-direction, in-plane shear strain, and curvature in the x-direction, respectively.

The generalize stress strain relationship is given by [25]:

$$\sigma_{ij}=c_{ijkl}\varepsilon_{kl} \tag{5}$$

where, $i,j=1,\cdots,6$; and $k=1,\cdots,3$.

The plane stress approximations are made by setting the stress component in the transverse direction $\sigma_{33}=0$, and eliminate the corresponding strain ε_{33} from the constitutive relation, Equation (5) as follows [25]:

Copyright © 2013 SciRes.

$$\begin{Bmatrix}\sigma_{11}\\ \sigma_{22}\\ \sigma_{23}\\ \sigma_{13}\\ \sigma_{12}\end{Bmatrix}_k = \begin{bmatrix} Q_{11} & Q_{12} & 0 & 0 & 0\\ Q_{12} & Q_{22} & 0 & 0 & 0\\ 0 & 0 & Q_{44} & 0 & 0\\ 0 & 0 & 0 & Q_{55} & 0\\ 0 & 0 & 0 & 0 & Q_{66}\end{bmatrix}_k \begin{Bmatrix}\varepsilon_{11}\\ \varepsilon_{22}\\ \varepsilon_{23}\\ \varepsilon_{13}\\ \varepsilon_{12}\end{Bmatrix}_k \quad (6)$$

where, Q_{ij} are the reduced stiffness components which related to the engineering constants for two material cases such as:

Case I: Isotropic Beam

$$Q_{11}^k = Q_{22}^k = \frac{E}{1-\nu^2}\ Q_{12}^k = \frac{\nu E}{1-\nu^2}\ Q_{44}^k = Q_{55}^k = Q_{66}^k = G \quad (7a)$$

where; E , G, and ν are the material properties.

Case II: Orthotropic Beam

$$Q_{11}^k = \frac{E_1^k}{1-\upsilon_{12}^k\upsilon_{21}^k}\quad Q_{12}^k = \frac{\upsilon_{12}^k E_2^k}{1-\upsilon_{12}^k\upsilon_{21}^k}\quad Q_{22}^k = \frac{E_2^k}{1-\upsilon_{12}^k\upsilon_{21}^k}\quad Q_{44}^k = G_{23}\ \ Q_{55}^k = G_{13}^k\ \ Q_{66}^k = G_{12}^k \quad (7b)$$

where; E_i is the modules in x_i direction, $G_{ij}\ (i \neq j)$ are the shear modules in the $x_i - x_j$ plane, and υ_{ij} are the associated Poisson's ratios.

Thus the transformed stress-strain relationship can be written as:

$$\begin{Bmatrix}\sigma_{xx}\\ \sigma_{yy}\\ \sigma_{yz}\\ \sigma_{xz}\\ \sigma_{xy}\end{Bmatrix}_k = \begin{bmatrix} \bar{Q}_{11} & \bar{Q}_{12} & 0 & 0 & \bar{Q}_{16}\\ \bar{Q}_{21} & \bar{Q}_{22} & 0 & 0 & \bar{Q}_{26}\\ 0 & 0 & \bar{Q}_{44} & \bar{Q}_{45} & 0\\ 0 & 0 & \bar{Q}_{45} & \bar{Q}_{55} & 0\\ \bar{Q}_{16} & \bar{Q}_{26} & 0 & 0 & \bar{Q}_{66}\end{bmatrix}_k \begin{Bmatrix}\varepsilon_{xx}\\ \varepsilon_{yy}\\ \gamma_{yz}\\ \gamma_{xz}\\ \gamma_{xy}\end{Bmatrix}_k \quad (8)$$

where, $\bar{Q}_{ij}$, are the transformed reduced stiffness components [25].

In the present model the width in y direction is stress free and a plane stress assumptions are used. Therefore, it is possible to set $\sigma_{yy} = \sigma_{yz} = \sigma_{xy} = \gamma_{yz} = \gamma_{xy} = 0$, and $\varepsilon_{yy} \neq 0$ in Equation (8). Therefore, the stress-strain relationship can be reduced to:

$$\begin{Bmatrix}\sigma_{xx}\\ \sigma_{xz}\end{Bmatrix} = \begin{bmatrix}\tilde{Q}_{11} & 0\\ 0 & k_s\tilde{Q}_{55}\end{bmatrix}\begin{Bmatrix}\varepsilon_{xx}\\ \gamma_{xz}\end{Bmatrix} \quad (9a)$$

where; k_s is the shear correction factor and the coefficients in Equation (9a) are given by:

Case I: Isotropic beam

$$\tilde{Q}_{11} = E\quad \tilde{Q}_{55} = G, \text{ and } \bar{Q}_{ij} = Q_{ij} \quad (9b)$$

Case II: Orthotropic Beam

$$\tilde{Q}_{11} = \bar{Q}_{11} - \frac{\bar{Q}_{12}\bar{Q}_{12}}{\bar{Q}_{22}}\quad \tilde{Q}_{55} = \bar{Q}_{55} \quad (9c)$$

3. Energy Formulation

The kinetic energy of the beam structure is given by [6]:

$$T = \frac{1}{2}\int_v \rho\left[\dot{u}^2 + \dot{w}^2\right]\mathrm{d}v \quad (10)$$

where, ρ is the mass density of the material of the beam.

The internal strain energy U for the beam structure is represented by [12]:

$$U = \frac{1}{2}\int_v \left(\sigma_{xx}\varepsilon_{xx} + \sigma_{xz}\gamma_{xz}\right)\mathrm{d}v \quad (11)$$

And the work done due to external loads is represented by [24]:

$$W = \int_0^L f_a u\mathrm{d}x + \int_0^L f_t w\mathrm{d}x + P_i w_i \quad (12)$$

where; f_a, and f_t are the transversal and axial forces along a surface with length L, respectively. P_i, is the concentrated force at point i and w_i is the corresponding generalized displacement.

Case I: Isotropic beam

By substituting Equations (9a), and (9b) into Equation (11), the internal strain energy is represented by:

$$U = \frac{1}{2}\int_v \left(E\varepsilon_{xx}^2 + k_s G\gamma_{xz}^2\right)\mathrm{d}v \quad (13)$$

By inserting Equations (3a), and (3b) into Equation (13), one can obtain:

$$U = \frac{1}{2}\int_v \left(E\left(\varepsilon_{xx}^\circ - z\kappa_{xx}^\circ\right)^2 + k_s G\left(-\phi_x + \frac{\mathrm{d}w_o}{\mathrm{d}x}\right)^2\right)\mathrm{d}v \quad (14a)$$

$$U = \frac{1}{2}\int_v \left(E\left(\left(\varepsilon_{xx}^\circ\right)^2 - \left(2z\varepsilon_{xx}^\circ\kappa_{xx}^\circ\right) + \left(z\kappa_{xx}^\circ\right)^2\right) + k_s G\left(\phi_x^2 - 2\phi_x\frac{\mathrm{d}w_o}{\mathrm{d}x} + \left(\frac{\mathrm{d}w_o}{\mathrm{d}x}\right)^2\right)\right)\mathrm{d}v \quad (14b)$$

Thus;

$$U = \frac{1}{2}\int_v \left(\left(E\left(\frac{\mathrm{d}u_o}{\mathrm{d}x}\right)^2 - 2zE\left(\left(\frac{\mathrm{d}u_o}{\mathrm{d}x}\right)\left(\frac{\mathrm{d}\phi_x}{\mathrm{d}x}\right)\right) + z^2E\left(\frac{\mathrm{d}\phi_x}{\mathrm{d}x}\right)^2\right) + k_s G\left(\phi_x^2 - 2\phi_x\frac{\mathrm{d}w_o}{\mathrm{d}x} + \left(\frac{\mathrm{d}w_o}{\mathrm{d}x}\right)^2\right)\right)\mathrm{d}v \quad (15)$$

Case II: Orthotropic Beam

By substituting Equation (9a) in Equation (11), the internal strain energy of the composite beam is represented by:

Copyright © 2013 SciRes.

$$U = \frac{1}{2}\int_v \left(\tilde{Q}_{11}\varepsilon_{xx}^2 + k_s\tilde{Q}_{55}\gamma_{xz}^2\right)\mathrm{d}v \tag{16}$$

By inserting Equations (3a), and (3b) into Equation (16), one can obtain:

$$U = \frac{1}{2}\int_v \left(\tilde{Q}_{11}\left(\varepsilon_{xx}^{\circ} - z\kappa_{xx}^{\circ}\right)^2 + k_s\tilde{Q}_{55}\left(-\phi_x + \frac{\mathrm{d}w_o}{\mathrm{d}x}\right)^2\right)\mathrm{d}v \tag{17a}$$

$$U = \frac{1}{2}\int_v \left(\tilde{Q}_{11}\left(\left(\varepsilon_{xx}^{\circ}\right)^2 - \left(2z\varepsilon_{xx}^{\circ}\kappa_{xx}^{\circ}\right) + \left(z\kappa_{xx}^{\circ}\right)^2\right) + k_s\tilde{Q}_{55}\left(\phi_x^2 - 2\phi_x\frac{\mathrm{d}w_o}{\mathrm{d}x} + \left(\frac{\mathrm{d}w_o}{\mathrm{d}x}\right)^2\right)\right)\mathrm{d}v \tag{17b}$$

And performing the integration through the thickness, the internal strain energy for anisotropic beam is represented by:

$$U = \frac{1}{2}\int_{-b/2}^{b/2}\int_0^L \left(A_{11}\left(\frac{\mathrm{d}u_o}{\mathrm{d}x}\right)^2 - 2B_{11}\left(\frac{\mathrm{d}u_o}{\mathrm{d}x}\right)\left(\frac{\mathrm{d}\phi_x}{\mathrm{d}x}\right) + D_{11}\left(\frac{\mathrm{d}\phi_x}{\mathrm{d}x}\right)^2 + k_s A_{55}\left(\phi_x^2 - 2\left(\phi_x\frac{\mathrm{d}w_o}{\mathrm{d}x}\right) + \left(\frac{\mathrm{d}w_o}{\mathrm{d}x}\right)^2\right)\right)\mathrm{d}x\mathrm{d}y \tag{18}$$

where, A_{ij}, B_{ij}, and D_{ij} are the laminate extensional, coupling, and bending stiffness coefficients and they are given by [25]:

$$\begin{aligned} A_{11} &= \int_{-h/2}^{h/2}\left(\tilde{Q}_{11}\right)_k \mathrm{d}z = \sum_{k=1}^{N}\left(\tilde{Q}_{11}\right)_k\left(z_k - z_{k-1}\right) \qquad A_{55} = \int_{-h/2}^{h/2}\left(\tilde{Q}_{55}\right)_k \mathrm{d}z = \sum_{k=1}^{N}\left(\tilde{Q}_{55}\right)_k\left(z_k - z_{k-1}\right) \\ B_{11} &= \int_{-h/2}^{h/2}\left(\tilde{Q}_{11}\right)_k z\mathrm{d}z = \frac{1}{2}\sum_{k=1}^{N}\left(\tilde{Q}_{11}\right)_k\left(z_k^2 - z_{k-1}^2\right) \quad D_{11} = \int_{-h/2}^{h/2}\left(\tilde{Q}_{11}\right)_k z^2\mathrm{d}z = \frac{1}{3}\sum_{k=1}^{N}\left(\tilde{Q}_{11}\right)_k\left(z_k^3 - z_{k-1}^3\right) \end{aligned} \tag{19}$$

4. Finite Element Formulation

In the present model the proposed element has five nodes with nine degrees of freedom representing the deformations $u, w,$ and ϕ_x as shown in the **Figure 2**.

A cubic shape functions are used to represent the axial displacement u, quadratic shape functions for the transverse displacement w, where the rotation ϕ_x is represented by a linear shape functions, this will result a nine by nine stiffness matrix with different degrees of freedom at different nodes [24]. From these selections we have:

$$\phi_x\left(\text{Linear}\right) \approx \frac{\mathrm{d}w_o}{\mathrm{d}x}\left(\text{Linear}\right), \text{ and}$$

$$\frac{\mathrm{d}u_o}{\mathrm{d}x}\left(\text{quadratic}\right) \approx \left(\frac{\mathrm{d}w_o}{\mathrm{d}x}\right)^2\left(\text{quadratic}\right)$$

Which satisfied the constrains, shear strain $\gamma_{xz}^0 \equiv \text{constant}$, and membrane strain $\varepsilon_{xx}^{\circ} \equiv 0$, to avoid the error in the finite element analysis which is known as shear Locking due to un-accurately models the curvature present in the actual material under bending, and a shear stress is introduced. The additional shear stress in the element causes the element to reach equilibrium with smaller displacement, *i.e.*, it makes the element appear to be stiffer than it actually is and gives bending displacements smaller than they should be. The axial displacement at the mid-plane u_0 is expressed as the following:

$$\frac{\partial^4 u_o}{\partial x^4} = 0 \tag{20}$$

By solving the previous equation and imposing the boundary conditions, the axial displacement can be represented as:

$$u_o\left(x\right) = u_1\xi_1 + u_2\xi_2 + u_3\xi_3 + u_4\xi_4 = \sum_{j=1}^{4} u_j\xi_j \tag{21}$$

where the cubic shape functions ξ_j are found to be [26]:

$$\begin{aligned} \xi_1 &= -\frac{9}{2}\left(\frac{x}{L}\right)^3 + 9\left(\frac{x}{L}\right)^2 - \frac{11}{2}\left(\frac{x}{L}\right) + 1 \\ \xi_2 &= \frac{27}{2}\left(\frac{x}{L}\right)^3 - \frac{45}{2}\left(\frac{x}{L}\right)^2 + 9\left(\frac{x}{L}\right) \\ \xi_3 &= \frac{-27}{2}\left(\frac{x}{L}\right)^3 + 18\left(\frac{x}{L}\right)^2 - \frac{9}{2}\left(\frac{x}{L}\right) \\ \xi_4 &= \frac{9}{2}\left(\frac{x}{L}\right)^3 - \frac{9}{2}\left(\frac{x}{L}\right)^2 + \frac{x}{L} \end{aligned} \tag{22}$$

The transversal displacement w is represented as:

$$\frac{\partial^3 w_o}{\partial x^3} = 0 \tag{23}$$

By solving the above equation and applying the boundary conditions to determine the unknown constants, the transversal displacement w can be expressed in terms of the nodal displacement as:

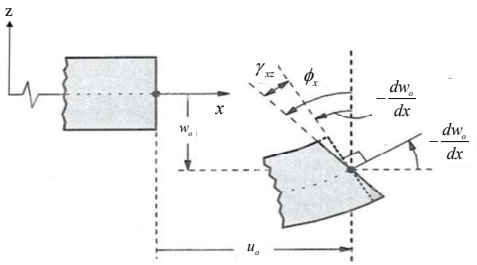

Figure 1. Deformed and un-deformed shape of Timoshenko beam [24].

Copyright © 2013 SciRes.

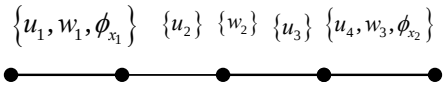

Figure 2. Element nodal degrees of freedom.

$$w_o(x) = w_1\zeta_1 + w_2\zeta_2 + w_3\zeta_3 = \sum_{j=1}^{3} w_j\zeta_j \tag{24}$$

where, the quadratic interpolation shape functions are given by [26]:

$$\begin{aligned}\zeta_1 &= 1-3\left(\frac{x}{L}\right)+2\left(\frac{x}{L}\right)^2\\ \zeta_2 &= 4\left(\frac{x}{L}\right)-4\left(\frac{x}{L}\right)^2\\ \zeta_3 &= -\left(\frac{x}{L}\right)+2\left(\frac{x}{L}\right)^2\end{aligned} \tag{25}$$

The rotation angle ϕ_x is expressed as:

$$\frac{\partial^2\phi_x}{\partial x^2} = 0 \tag{26}$$

Similarly; by solving Equation (26) and applying the boundary conditions, the rotation angle is given by:

$$\phi_x(x) = \phi_{x1}\psi_1 + \phi_{x2}\psi_2 = \sum_{j=1}^{2}\phi_{xj}\psi_j \tag{27}$$

where the Linear interpolation shape functions ψ_j have the form [27]:

$$\psi_1 = 1-\frac{x}{L}, \text{ and } \psi_2 = \frac{x}{L} \tag{28}$$

5. Variational Formulation

The mathematical statement of Hamilton's principle can be expressed as [3]:

$$\int_{t_1}^{t_2}\left(\delta(T-U)+\delta W\right)\mathrm{d}t = 0 \tag{29}$$

where, δ denote the first variation, t_1 and t_2 are two arbitrary time variables except that at $t = t_1$, and $t = t_2$, all variation are zero. The advantage of this method is that it accounts for the physics of the entire structure simultaneously. Starting with the first integral and assume that each layer of the present composite beam model has the same vibration speed.

Thus the first variation of the kinetic energy Equation (10) is expressed as:

$$\delta T = -\int_v \rho\left(\ddot{u}\delta u + \ddot{w}\delta w\right)\mathrm{d}v \tag{30}$$

By inserting Equation (2) into Equation (30) yields:

$$\delta T = -\int_v \rho\left[\left(\delta u_o^T\ddot{u}_o - z\delta u_o^T\ddot{\phi}_x - z\delta\phi_x^T\ddot{u}_o + z^2\delta\phi_x^T\ddot{\phi}_x\right)+\left(\delta w_o^T\ddot{w}_o\right)\right]\mathrm{d}v \tag{31}$$

By substituting the shape functions Equations. (21), (24), and (27) in Equation (31) the components of the element mass matrix can be expressed by:

$$\begin{aligned}&M_{11} = I_0\int_0^L[\xi_i]^T[\xi_i]\mathrm{d}x \;\; i=1,\cdots,4 \quad M_{12}=0 \;\; M_{13} = -I_1\int_0^L[\xi_i]^T[\psi_j]\mathrm{d}x \quad i=1,\cdots,4 \text{ and } j=1,2\\ &M_{21}=0 \; M_{22} = I_0\int_0^L[\zeta_i]^T[\zeta_i]\mathrm{d}x \; i=1,\cdots,3 \;\; M_{23}=0 \quad M_{31} = -I_1\int_0^L[\psi_i]^T[\xi_j]\mathrm{d}x \;\; i=1,2 \text{ and } j=1,\cdots,4\\ &M_{32}=0 \;\; M_{33} = I_2\int_0^L[\psi_i]^T[\psi_i]\mathrm{d}x \;\; i=1,2 \;\text{ and }\; (I_0,I_1,I_2) = \rho\int_A(1,z,z^2)\mathrm{d}A\end{aligned} \tag{32}$$

where, I_i is the mass moment of inertia.

By inserting Equations (22), (25), and (28) into Equation (32) and perform the integrating, the element mass matrix is obtained, and given in Appendix A.

The first variation of the external work Equation (12) takes the form:

$$\delta W = \int_0^L f_a\left(\delta u_o - z\delta\phi_x\right)\mathrm{d}x + \int_0^L f_t\delta w_o\mathrm{d}x + P_i\delta w_{o_i} \tag{33}$$

By inserting the shape functions Equations. (21), (24), and (27) into Equation (33), one can obtain:

$$\begin{aligned}\delta W = &\int_0^L f_a\xi_i\delta u_{oi}\mathrm{d}x - \int_0^L f_a\psi_i z\delta\phi_{xi}\mathrm{d}x\\ &+\int_0^L f_t\zeta_i\delta w_{oi}\mathrm{d}x + P_i\end{aligned} \tag{34}$$

Thus, the elements of the load vector are as follows:

$$\begin{aligned}&F_{11} = \int_0^L f_a\xi_1\mathrm{d}x \quad F_{12} = \int_0^L f_a\xi_2\mathrm{d}x \quad F_{13} = \int_0^L f_a\xi_3\mathrm{d}x \quad F_{14} = \int_0^L f_a\xi_4\mathrm{d}x \quad F_{21} = P_1 + \int_0^L f_t\zeta_1\mathrm{d}x\\ &F_{22} = P_2 + \int_0^L f_t\zeta_2\mathrm{d}x \quad F_{23} = P_3 + \int_0^L f_t\zeta_3\mathrm{d}x \quad F_{31} = -\int_0^L f_a z\psi_1\mathrm{d}x \quad F_{32} = -\int_0^L f_a z\psi_2\mathrm{d}x\end{aligned} \tag{35}$$

Copyright © 2013 SciRes.

By substituting Equations (22), (25), and (28) in Equation (35) and perform the integrating, the element load vector can be obtained and given in Appendix A.

Case I: Isotropic beam:

By taking the variation of Equation (15), one can obtain:

$$\begin{aligned}\delta U = \frac{1}{2}\int_v \Bigg[& 2E\left(\sum_{j=1}^{4}\left(\frac{\mathrm{d}u_{oj}}{\mathrm{d}x}\right)\sum_{i=1}^{4}\left(\frac{\delta \mathrm{d}u_{oi}}{\mathrm{d}x}\right)\right) - 2Ez\left(\left(\sum_{j=1}^{2}\left(\frac{\mathrm{d}\phi_{xj}}{\mathrm{d}x}\right)\sum_{i=1}^{4}\left(\frac{\delta \mathrm{d}u_{oi}}{\mathrm{d}x}\right)\right)+\left(\sum_{j=1}^{4}\left(\frac{\mathrm{d}u_{oj}}{\mathrm{d}x}\right)\sum_{i=1}^{2}\left(\frac{\delta \mathrm{d}\phi_{xi}}{\mathrm{d}x}\right)\right)\right)\\ & + 2Ez^2\left(\sum_{j=1}^{2}\left(\frac{\mathrm{d}\phi_{xj}}{\mathrm{d}x}\right)\sum_{i=1}^{2}\left(\frac{\delta \mathrm{d}\phi_{xi}}{\mathrm{d}x}\right)\right) + 2k_sG\left(\left(\sum_{j=1}^{2}\left(\phi_{xj}\right)\sum_{i=1}^{2}\left(\delta\phi_{xi}\right)\right)-\left(\sum_{j=1}^{2}\left(\phi_{xj}\right)\sum_{i=1}^{3}\left(\frac{\delta \mathrm{d}w_{oi}}{\mathrm{d}x}\right)\right)\right)\\ & -\left(\sum_{j=1}^{3}\left(\frac{\mathrm{d}w_{oj}}{\mathrm{d}x}\right)\sum_{i=1}^{2}\left(\delta\phi_{xi}\right)\right)+\left(\sum_{j=1}^{3}\left(\frac{\mathrm{d}w_{oj}}{\mathrm{d}x}\right)\sum_{i=1}^{3}\left(\frac{\delta \mathrm{d}w_{oi}}{\mathrm{d}x}\right)\right)\Bigg]\mathrm{d}v\end{aligned} \tag{36}$$

By substituting Equations (21), (24) and (27) in Equation (36) yields:

$$\begin{aligned}\delta U = \frac{1}{2}\int_v \Bigg[& 2E\left(\sum_{j=1}^{4}\left(\frac{\mathrm{d}\xi_{j}}{\mathrm{d}x}\right)\sum_{i=1}^{4}\left(\frac{\delta \mathrm{d}\xi_{i}}{\mathrm{d}x}\right)\right) - 2Ez\left(\left(\sum_{j=1}^{2}\left(\frac{\mathrm{d}\psi_{j}}{\mathrm{d}x}\right)\sum_{i=1}^{4}\left(\frac{\delta \mathrm{d}\xi_{i}}{\mathrm{d}x}\right)\right)+\left(\sum_{j=1}^{4}\left(\frac{\mathrm{d}\xi_{j}}{\mathrm{d}x}\right)\sum_{i=1}^{2}\left(\frac{\delta \mathrm{d}\psi_{i}}{\mathrm{d}x}\right)\right)\right)\\ & + 2Ez^2\left(\sum_{j=1}^{2}\left(\frac{\mathrm{d}\psi_{j}}{\mathrm{d}x}\right)\sum_{i=1}^{2}\left(\frac{\delta \mathrm{d}\psi_{i}}{\mathrm{d}x}\right)\right) + 2k_sG\left(\left(\sum_{j=1}^{2}\left(\psi_{j}\right)\sum_{i=1}^{2}\left(\delta\psi_{i}\right)\right)-\left(\sum_{j=1}^{2}\left(\psi_{j}\right)\sum_{i=1}^{3}\left(\frac{\delta \mathrm{d}\zeta_{i}}{\mathrm{d}x}\right)\right)\right)\\ & -\left(\sum_{j=1}^{3}\left(\frac{\mathrm{d}\zeta_{j}}{\mathrm{d}x}\right)\sum_{i=1}^{2}\left(\delta\psi_{i}\right)\right)+\left(\sum_{j=1}^{3}\left(\frac{\mathrm{d}\zeta_{j}}{\mathrm{d}x}\right)\sum_{i=1}^{3}\left(\frac{\delta \mathrm{d}\zeta_{i}}{\mathrm{d}x}\right)\right)\Bigg]\mathrm{d}v\end{aligned} \tag{37}$$

Equation (37) defines the elements of the stiffness matrix as follows:

$$\begin{aligned}
&k_{11} = E\int_v\left(\sum_{i=1}^{4}\left(\frac{\mathrm{d}\xi_i}{\mathrm{d}x}\right)\sum_{j=1}^{4}\left(\frac{\mathrm{d}\xi_j}{\mathrm{d}x}\right)\right)\mathrm{d}v \quad k_{12}=k_{21} \quad k_{13} = -\int_v Ez\left(\sum_{i=1}^{4}\left(\frac{\mathrm{d}\xi_i}{\mathrm{d}x}\right)\sum_{j=1}^{2}\left(\frac{\mathrm{d}\psi_j}{\mathrm{d}x}\right)\right)\mathrm{d}v \quad k_{22} = k_sG\int_v\left(\sum_{i=1}^{3}\left(\frac{\mathrm{d}\zeta_i}{\mathrm{d}x}\right)\sum_{j=1}^{3}\left(\frac{\mathrm{d}\zeta_j}{\mathrm{d}x}\right)\right)\mathrm{d}v\\
&k_{23} = -k_sG\int_v\left(\sum_{i=1}^{3}\left(\frac{\mathrm{d}\zeta_i}{\mathrm{d}x}\right)\sum_{j=1}^{2}\left(\psi_j\right)\right)\mathrm{d}v \quad k_{31} = -Ez\int_v\left(\sum_{i=1}^{2}\left(\frac{\mathrm{d}\psi_i}{\mathrm{d}x}\right)\sum_{j=1}^{4}\left(\frac{\mathrm{d}\xi_j}{\mathrm{d}x}\right)\right)\mathrm{d}v \quad k_{32} = -k_sG\int_v\left(\sum_{i=1}^{2}\left(\psi_i\right)\sum_{j=1}^{3}\left(\frac{\mathrm{d}\zeta_j}{\mathrm{d}x}\right)\right)\mathrm{d}v\\
&k_{11} = E\int_v\left(\sum_{i=1}^{4}\left(\frac{\mathrm{d}\xi_i}{\mathrm{d}x}\right)\sum_{j=1}^{4}\left(\frac{\mathrm{d}\xi_j}{\mathrm{d}x}\right)\right)\mathrm{d}v \quad k_{12}=k_{21} \quad k_{13} = -\int_v Ez\left(\sum_{i=1}^{4}\left(\frac{\mathrm{d}\xi_i}{\mathrm{d}x}\right)\sum_{j=1}^{2}\left(\frac{\mathrm{d}\psi_j}{\mathrm{d}x}\right)\right)\mathrm{d}v \quad k_{22} = k_sG\int_v\left(\sum_{i=1}^{3}\left(\frac{\mathrm{d}\zeta_i}{\mathrm{d}x}\right)\sum_{j=1}^{3}\left(\frac{\mathrm{d}\zeta_j}{\mathrm{d}x}\right)\right)\mathrm{d}v\\
&k_{23} = -k_sG\int_v\left(\sum_{i=1}^{3}\left(\frac{\mathrm{d}\zeta_i}{\mathrm{d}x}\right)\sum_{j=1}^{2}\left(\psi_j\right)\right)\mathrm{d}v \quad k_{31} = -Ez\int_v\left(\sum_{i=1}^{2}\left(\frac{\mathrm{d}\psi_i}{\mathrm{d}x}\right)\sum_{j=1}^{4}\left(\frac{\mathrm{d}\xi_j}{\mathrm{d}x}\right)\right)\mathrm{d}v \quad k_{32} = -k_sG\int_v\left(\sum_{i=1}^{2}\left(\psi_i\right)\sum_{j=1}^{3}\left(\frac{\mathrm{d}\zeta_j}{\mathrm{d}x}\right)\right)\mathrm{d}v
\end{aligned} \tag{38}$$

By inserting Equation (22), (25) and (28) into Equation (38), and perform the integration, the element stiffness matrix for isotropic Timoshenko Beam is obtained and given in Appendix A.

Case II: Orthotropic Beam:

By taking the variation of Equation (18), one can obtain:

$$\begin{aligned}\delta U = \frac{1}{2}\int_{-b/2}^{b/2}\int_{0}^{L} \Bigg[& 2A_{11}\left(\sum_{j=1}^{4}\left(\frac{\mathrm{d}\xi_{j}}{\mathrm{d}x}\right)\sum_{i=1}^{4}\left(\frac{\delta \mathrm{d}\xi_{i}}{\mathrm{d}x}\right)\right) - 2B_{11}\left(\left(\sum_{j=1}^{2}\left(\frac{\mathrm{d}\psi_{j}}{\mathrm{d}x}\right)\sum_{i=1}^{4}\left(\frac{\delta \mathrm{d}\xi_{i}}{\mathrm{d}x}\right)\right)+\left(\sum_{j=1}^{4}\left(\frac{\mathrm{d}\xi_{j}}{\mathrm{d}x}\right)\sum_{i=1}^{2}\left(\frac{\delta \mathrm{d}\psi_{i}}{\mathrm{d}x}\right)\right)\right)\\ & + 2D_{11}\left(\sum_{j=1}^{2}\left(\frac{\mathrm{d}\psi_{j}}{\mathrm{d}x}\right)\sum_{i=1}^{2}\left(\frac{\delta \mathrm{d}\psi_{i}}{\mathrm{d}x}\right)\right) + 2k_sA_{55}\left(\left(\sum_{j=1}^{2}\left(\psi_{j}\right)\sum_{i=1}^{2}\left(\delta\psi_{i}\right)\right)-\left(\sum_{j=1}^{2}\left(\psi_{j}\right)\sum_{i=1}^{3}\left(\frac{\delta \mathrm{d}\zeta_{i}}{\mathrm{d}x}\right)\right)\right)\\ & -\left(\sum_{j=1}^{3}\left(\frac{\mathrm{d}\zeta_{j}}{\mathrm{d}x}\right)\sum_{i=1}^{2}\left(\delta\psi_{i}\right)\right)+\left(\sum_{j=1}^{3}\left(\frac{\mathrm{d}\zeta_{j}}{\mathrm{d}x}\right)\sum_{i=1}^{3}\left(\frac{\delta \mathrm{d}\zeta_{i}}{\mathrm{d}x}\right)\right)\Bigg]\mathrm{d}x\mathrm{d}y\end{aligned} \tag{39}$$

By inserting Equations (21), (24) and (27) into Equation (39) yields the form given in Equation (40):

The element stiffness matrix can be deduced from Equation (40) as shown in Equation (41):

Copyright © 2013 SciRes.

By substituting Equation (22), (25) and (28) in Equation (41) and perform the integration, the element stiffness matrix of anisotropic Timoshenko beam is obtained and given in Appendix A.

6. Equation of Motion

The system equation of motion is given in matrix form as [11]:

$$[M]\{\ddot{q}\}+[K]\{q\}=\{F\} \tag{42}$$

where $[M]$ is the global mass matrix, $\{\ddot{q}\}$ is the second derivative of the nodal displacements with respect to time, $[K]$ is the global stiffness matrix, $\{q\}$ is the nodal displacements vector and $\{F\}$ is the global nodal forces vector.

7. Numerical Example and Discussion

A MATLAB code is constructed to perform the analysis of isotropic and orthotropic beams using the present finite element model. The model is capable of predicting the nodal (axial and transversal) deflections and the fundamental natural frequency of the beam. The model inputs are the materials and geometric properties of the beams. The shear correction factor is taken as k = 5/6, and the following boundary conditions of the beams are considered as follows:

Simply-supported edge: $u=0,$ and $w=0$.

Clamped edge: $u=0$, $w=0$, and $\phi_x=0$.

The model validation is performed by checking the convergences for deflection and eigen-values, static deflections and dynamic characteristics for both isotropic and orthotropic beams.

Case I: Isotropic beam results

1) Model Convergences

The convergence of the present model is checked for the aluminum beam with the material and geometric properties given in **Table 1**. The beam is subjected to uniform distributed load of intensity 1 N/m. The obtained results are shown in **Figure 3**, which presents the effect of number of element on the normalized transversal tip deflection of a cantilever beam, with length to height ratio (L/h) of 10, The normalized deflection is given as; $\bar{w}=w10^2/EI_{yy}L^4$. It can be seen from the figure that the model predictions are start to converge at reasonable number of elements.

The convergence of the Eigen values is checked for two cases of the beam boundary conditions clamped-free and clamped-clamped where the dimensionless frequency $\bar{\omega}$ is defined as: $\bar{\omega}_i^2=\omega_i L^2\sqrt{\frac{m}{EI}}$, and m is the mass per unit length of the beam.

a) Clamped-free aluminum beam with the properties given in **Table 1**. The obtained dimensionless first natural frequency is conversing by increasing the number of elements as shown in **Figure 4**.

b) Clamped-Clamped aluminum beam with the properties: Poisson's ratio $\nu=0.3$ thickness to length ratio is h/L=0.01, and the number of elements are chosen from 10 to 40. The obtained normalized natural frequencies are presented in **Table 2** for different number of ele-

$$\begin{aligned}\delta U=\frac{1}{2}\int_{-b/2}^{b/2}\int_0^L\Bigg[&2A_{11}\left(\sum_{j=1}^{4}\left(\frac{\mathrm{d}\xi_j}{\mathrm{d}x}\right)\sum_{i=1}^{4}\left(\frac{\delta\mathrm{d}\xi_i}{\mathrm{d}x}\right)\right)-2B_{11}\left(\left(\sum_{j=1}^{2}\left(\frac{\mathrm{d}\psi_j}{\mathrm{d}x}\right)\sum_{i=1}^{4}\left(\frac{\delta\mathrm{d}\xi_i}{\mathrm{d}x}\right)\right)+\left(\sum_{j=1}^{4}\left(\frac{\mathrm{d}\xi_j}{\mathrm{d}x}\right)\sum_{i=1}^{2}\left(\frac{\delta\mathrm{d}\psi_i}{\mathrm{d}x}\right)\right)\right)\\&+2D_{11}\left(\sum_{j=1}^{2}\left(\frac{\mathrm{d}\psi_j}{\mathrm{d}x}\right)\sum_{i=1}^{2}\left(\frac{\delta\mathrm{d}\psi_i}{\mathrm{d}x}\right)\right)+2k_sA_{55}\left(\left(\sum_{j=1}^{2}\left(\psi_j\right)\sum_{i=1}^{2}\left(\delta\psi_i\right)\right)-\left(\sum_{j=1}^{2}\left(\psi_j\right)\sum_{i=1}^{3}\left(\frac{\delta\mathrm{d}\zeta_i}{\mathrm{d}x}\right)\right)\right.\\&\left.-\left(\sum_{j=1}^{3}\left(\frac{\mathrm{d}\zeta_j}{\mathrm{d}x}\right)\sum_{i=1}^{2}\left(\delta\psi_i\right)\right)+\left(\sum_{j=1}^{3}\left(\frac{\mathrm{d}\zeta_j}{\mathrm{d}x}\right)\sum_{i=1}^{3}\left(\frac{\delta\mathrm{d}\zeta_i}{\mathrm{d}x}\right)\right)\right)\Bigg]\mathrm{d}x\mathrm{d}y\end{aligned} \tag{40}$$

$$\begin{aligned}&k_{11}=A_{11}\int_{-b/2}^{b/2}\int_0^L\left(\sum_{i=1}^{4}\left(\frac{\mathrm{d}\xi_i}{\mathrm{d}x}\right)\sum_{j=1}^{4}\left(\frac{\mathrm{d}\xi_j}{\mathrm{d}x}\right)\right)\mathrm{d}x\mathrm{d}y\quad k_{12}=k_{21}\quad k_{13}=-B_{11}\int_{-b/2}^{b/2}\int_0^L\left(\sum_{i=1}^{4}\left(\frac{\mathrm{d}\xi_i}{\mathrm{d}x}\right)\sum_{j=1}^{2}\left(\frac{\mathrm{d}\psi_j}{\mathrm{d}x}\right)\right)\mathrm{d}x\mathrm{d}y\\&k_{22}=k_sA_{55}\int_{-b/2}^{b/2}\int_0^L\left(\sum_{i=1}^{3}\left(\frac{\mathrm{d}\zeta_i}{\mathrm{d}x}\right)\sum_{j=1}^{3}\left(\frac{\mathrm{d}\zeta_j}{\mathrm{d}x}\right)\right)\mathrm{d}x\mathrm{d}y\quad k_{23}=-k_sA_{55}\int_{-b/2}^{b/2}\int_0^L\left(\sum_{i=1}^{3}\left(\frac{\mathrm{d}\zeta_i}{\mathrm{d}x}\right)\sum_{j=1}^{2}\left(\psi_j\right)\right)\mathrm{d}x\mathrm{d}y\\&k_{31}=-B_{11}\int_{-b/2}^{b/2}\int_0^L\left(\sum_{i=1}^{2}\left(\frac{\mathrm{d}\psi_i}{\mathrm{d}x}\right)\sum_{j=1}^{4}\left(\frac{\mathrm{d}\xi_j}{\mathrm{d}x}\right)\right)\mathrm{d}x\mathrm{d}y\quad k_{32}=-k_sA_{55}\int_{-b/2}^{b/2}\int_0^L\left(\sum_{i=1}^{2}\left(\psi_i\right)\sum_{j=1}^{3}\left(\frac{\mathrm{d}\zeta_j}{\mathrm{d}x}\right)\right)\mathrm{d}x\mathrm{d}y\\&k_{33}=\int_{-b/2}^{b/2}\int_0^L\left(D_{11}\sum_{i=1}^{2}\left(\frac{\mathrm{d}\psi_i}{\mathrm{d}x}\right)\sum_{j=1}^{2}\left(\frac{\mathrm{d}\psi_j}{\mathrm{d}x}\right)+k_sA_{55}\sum_{i=1}^{2}\left(\psi_i\right)\sum_{j=1}^{2}\left(\psi_j\right)\right)\mathrm{d}x\mathrm{d}y\end{aligned} \tag{41}$$

Copyright © 2013 SciRes.

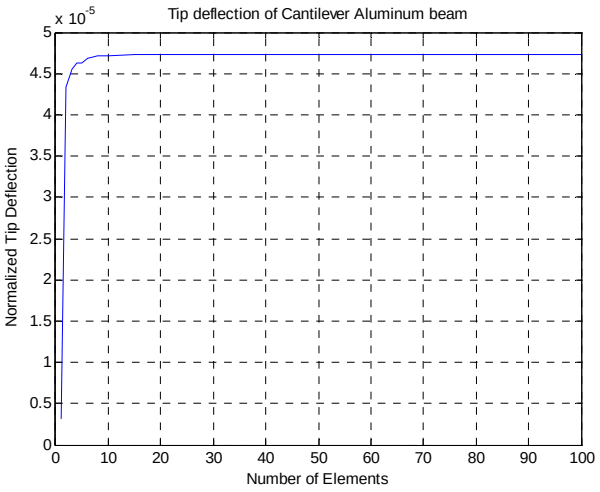

Figure 3. Normalized transversal tip displacements vs. number of elements of cantilever aluminum beam.

Table 1. Material and geometric properties for aluminum beam.

Property	Aluminum	Unit
E	68.9	GPa
V	0.25	-
G	27.6	GPa
ρ	2769	(kg/m^3)
Length, L	0.1524	(m)
Width, b	0.0254	(m)
Height, h	0.01524	(m)

ments "NE". The obtained results are found reasonable and compared with the predictions given by [16], which used different numbers of collocation points to determine the size of the problem in their studies It is clear from **Figure 4** and **Table 2** that as the number of elements increase the natural frequency decreases for the first and other modes.

2) Static Validation

Example (1):

A cantilever isotropic beam with cross-section dimensions $h = b = 1$, $E = 1$, and $\upsilon = 1$ are used in the validation in order to compared with other references. The beam is subjected to transverse uniform distributed loads with intensity $f_t = 1$ up to 10 N/m, and with different values of length to thickness ratio L/h = 4, 10, 20, 50, and 100. In the present example, the shear correction factor is taken as $k_s = 5/6$ and number of elements, NE = 33, are taken in the proposed model in order to compare the results to other references. The obtained results are presented and in **Table 3(a)-(e)** and compared to [3], where the Timoshenko–based tip deflection

is given as: $W_t = \dfrac{f_t L^4}{8EI_{yy}}\left(1+\bar{\varphi}\right)$, $\bar{\varphi} = \dfrac{1}{5}\left(12+11\upsilon\right)\left(\dfrac{h}{2}\right)^2$, and its shear correction factor is $k_s = \dfrac{10\left(1+\upsilon\right)}{12+11\upsilon}$. Also compared with the known Euler formula for max tip deflection, $W_{\max} = f_t L^4 / 8EI_{yy}$.

It is shown from the previous tables that for L/h less than 20 the proposed model gives results more accurate then the exact formula of Timoshenko and Euler beams. For L/h greater than 20 the values of the obtained results are start to be less than Timoshenko based solution and gradually get closer to Euler solution.

Example (2):

A cantilever beam with the following properties: $E = 29000$, $b = 1$, $\upsilon = 0.3$ subjected to tip load $P = 100$ as given by [15]. It is shown from the obtained results given in **Table 4** the following: 1) the model accuracy is in between the HSDT and the finite element and other different solutions; 2) also the effect of the shear correction factor on the obtained results.

3) Dynamic Validation

The free vibration validation is performed for the aluminum beam with material properties given in **Table 1**. The obtained results are given in **Table 5**. to **Table 7**. for beams with different boundary conditions with NE = 35 and the ratio h/L = 0.002 to 0.2. The obtained dimensionless frequencies $\bar{\omega}$ are compared with the previously published results of CBT [28], FSDT [29], TSDT [18], and CPM [16].

For clamped-clamped beam, **Table 5(a)** shows the following for the first five modes:

1) For h/L = 0.2, the present model results are better than TODT but less than FSDT, and CPM.

2) For h/L less than or equal 0.1, the present model is less than all other theories.

Table 5(b) shows the following for the next five modes (6 - 10):

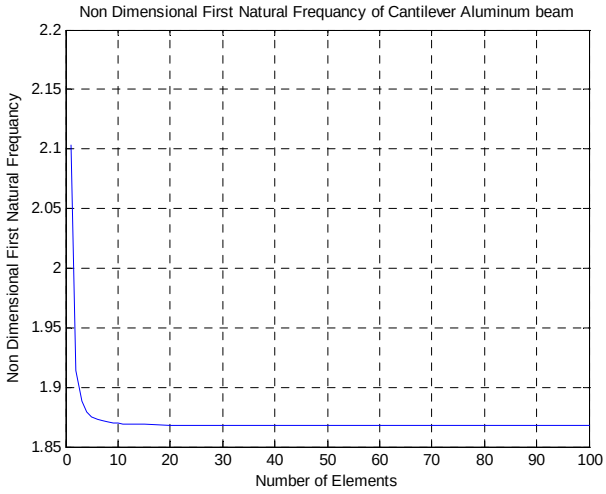

Figure 4. Non-dimensional first natural frequency vs. number of elements of cantilever aluminum beam.

Copyright © 2013 SciRes.

Table 2. Convergence test of the non-dimensional frequency $\bar{\omega}$ of clamped-clamped aluminum beam with the number of elements.

Mode	NE = 10	NE = 15	NE = 20	NE = 25	NE = 30	NE = 35	NE = 40
1	4.7782	4.7502	4.7406	4.7362	4.7338	4.7324	4.7314
2	8.0324	7.9274	7.8918	7.8755	7.8667	7.8615	7.8580
3	11.4368	11.1751	11.0883	11.0489	11.0277	11.0150	11.0068
4	15.0259	14.4920	14.3190	14.2411	14.1994	14.1745	14.1584
5	18.8565	17.8984	17.5937	17.4580	17.3856	17.3424	17.3146
6	22.9619	21.4145	20.9217	20.7043	20.5890	20.5203	20.4762
7	27.2381	25.0601	24.3123	23.9850	23.8122	23.7098	23.6439
8	31.0663	28.8515	27.7749	27.3049	27.0581	26.9122	26.8186
9	32.9891	32.7919	31.3183	30.6690	30.3294	30.1291	30.0011
10	46.6536	32.9891	32.9891	32.9891	32.9891	32.9891	32.9891
11	57.1389	36.8493	34.9500	34.0819	33.6285	33.3621	33.1919
12	65.2975	40.9061	38.6739	37.5477	36.9581	36.6123	36.3920
13	65.3674	44.6623	42.4870	41.0701	40.3205	39.8813	39.6018
14	65.9788	46.6536	46.3727	44.6510	43.7176	43.1701	42.8222
15	73.7684	47.5118	46.6536	46.6536	46.6536	46.4798	46.0535
16	80.8143	57.1388	50.2883	48.2902	47.1511	46.6536	46.6536
17	84.5794	65.9782	54.1445	51.9835	50.6216	49.8114	49.2964
18	87.3015	73.7661	57.1388	55.7200	54.1291	53.1652	52.5511
19	89.2551	80.1672	57.7730	57.1388	57.1388	56.5415	55.8179
20	93.3538	80.1711	60.8863	59.4787	57.6717	57.1388	57.1388
21	94.5830	80.8072	63.0643	63.2219	61.2454	59.9399	59.0968
22	99.0611	87.2829	65.9782	65.9782	64.8425	63.3593	62.3876
23	99.9947	93.3119	73.7659	66.8859	65.9782	65.9782	65.6899
24	104.6635	98.9770	80.8066	70.3684	68.4508	66.7974	65.9782
25	105.3547	102.1423	87.2813	73.5113	72.0505	70.2507	69.0028

1) For h/L equal to or grater than 0.1, the present model is gives more accurate results than all theories by significant values, and this difference increase by increasing the mode number.

2) For all modes as the ratio h/L increases the natural frequencies decreases.

Table 6(a) shows the first five modes of Free-Free beam it is clear that:

1) As long as h/L less than or equal to 0.05 the obtained results are closed to CBT and CBM theories.

2) For h/L greater than or equal to 0.05 the model results are better than other theories.

Table 6(b) shows the next five modes (6 - 10), for F-F beam as long as h/L less than 0.05 the proposed model gives less accuracy than CPM and CBT theories. For the ratio L/h less than or equal 0.05 the model results are better than CPM theory.

It seen from **Table 7(a)** for the first five modes of the S-S beam the proposed model gives results closer to all other theories for all values of h/L.

Table 7(b) shows the modes 6 to 10 for S-S beam it is clear that as long as h/L less than or equal to 0.02, the proposed model gives results closed to other theories. For the ratio h/L greater than or equal 0.05 the model results are better than all other theories with remarkable values.

CASE II: Orthotropic Beam Results

a) Model convergences

The convergence of the present model is checked for the orthotropic beam with the material properties given as; $E_1/E_2 = 25$, $G_{13} = G_{12} = 0.5E_2$, $G_{23} = 0.2E_2$, $\rho = 1$, and $\nu_{12} = 0.25$. A cantilever composite beams with different orientation angles [45/-45/45/-45], [30/50/30/50], and [0/90/0/90] with length to height ratio (L/h) is equal to 10, are used. The beam is subjected to uniform distributed load f_t of intensity 1 N/m. **Figure 5** shows the effect of number of element on the normalized transversal

Copyright © 2013 SciRes.

Table 3. (a) Transverse tip deflection of isotropic cantilever beam for different values of applied loads (L/h = 4); (b) Transverse tip deflection of isotropic cantilever beam for different values of applied loads (L/h = 10); (c) Transverse tip deflection of isotropic cantilever beam for different values of applied loads (L/h = 20); (d) Transverse tip deflection of isotropic cantilever beam for different values of applied loads (L/h = 50); (e) Transverse tip deflection of isotropic cantilever beam for different values of applied loads (L/h = 100).

(a)

f_t	Proposed Model	Exact Timoshenko [3]	Euler Theory
1	408.8425	408.8400	384
2	817.6849	816.9600	768
3	1.2265e+003	1.2254e+003	1152
4	1.6354e+003	1.6339e+003	1536
5	2.0442e+003	2.0424e+003	1920
6	2.4531e+003	2.4509e+003	2304
7	2.8619e+003	2.8594e+003	2688
8	3.2707e+003	3.2678e+003	3072
9	3.6796e+003	3.6763e+003	3456
10	4.0884e+003	4.0848e+003	3840

(b)

f_t	Proposed Model	Exact Timoshenko [3]	Euler Theory
1	1.5151e+004	1.5153e+004	1.5000e+004
2	3.0303e+004	3.0306e+004	3.0000e+004
3	4.5454e+004	4.5456e+004	4.5000e+004
4	6.0606e+004	6.0612e+004	6.0000e+004
5	7.5757e+004	7.5765e+004	7.5000e+004
6	9.0908e+004	9.0918e+004	9.0000e+004
7	1.0606e+004	1.06071e+005	1.0500e+005
8	1.2121e+005	1.21224e+005	1.2000e+005
9	1.3636e+005	1.36377e+005	1.3500e+005
10	1.5151e+005	1.51530e+005	1.5000e+005

(c)

f_t	Proposed Model	Exact Timoshenko [3]	Euler Theory
1	2.4055e+005	2.40612e+005	2.4000e+005
2	4.8110e+005	4.81224e+005	4.8000e+005
3	7.2165e+005	7.21836e+005	7.2000e+005
4	9.6220e+005	6.92448e+005	9.6000e+005
5	1.2028e+006	1.203060e+006	1.2000e+005
6	1.4433e+006	1.443672e+006	1.4400e+005
7	1.6839e+006	1.684284e+006	1.6800e+005
8	1.9244e+006	1.924896e+006	1.9200e+005
9	2.1650e+006	2.165508e+006	2.1600e+005
10	2.4055e+006	2.406120e+006	2.4000e+005

(d)

f_t	Proposed Model	Exact Timoshenko [3]	Euler Theory
1	9.3760e+006	9378825	9.3750e+006
2	1.8752e+007	18757650	1.8750+007
3	2.8128e+007	28136475	2.8125e+007
4	3.7504e+007	37515300	3.7500e+007
5	4.6880e+007	46894125	4.6875e+007
6	5.6256e+007	56272950	5.6250e+007
7	6.5632e+007	65651775	6.5625e+007
8	7.5008e+007	75030600	7.5000e+007
9	8.4384e+007	84409425	8.4375e+007
10	9.3760e+007	93788250	9.3750e+007

Copyright © 2013 SciRes.

(e)

f_t	Proposed Model	Exact Timoshenko [3]	Euler Theory
1	1.4997e+008	1.5002e+008	1.5000e+008
2	2.9994e+008	3.0003e+008	3.0000e+008
3	4.4991e+008	4.5005e+008	4.5000e+008
4	5.9988e+008	6.0006e+008	6.0000e+008
5	7.4985e+008	7.5008e+008	7.5000e+008
6	8.9982e+008	9.0009e+008	9.0000e+008
7	1.0498e+009	1.0501e+009	1.0500e+009
8	1.1998e+009	1.2001e+009	1.2000e+009
9	1.3497e+009	1.3501e+009	1.3500e+009
10	1.4997e+009	1.5002e+009	1.5000e+009

Table 4. Transverse tip deflection of isotropic cantilever beam compared with other theories.

L	h	Proposed Model $k_s = 5/6$	Timoshenko Theory*	Timoshenko Theory $k_s = 5/6$	Euler Theory	HSDT [15]	FE [28]	Elasticity Solution [15]
160	**12**	32.8307	32.8355	32.8382	32.6948	32.8376	32.823	32.8741
80		4.1576	4.1572	4.1586	4.0868	4.1587	4.1567	4.17650
40		0.5466	0.5460	0.5467	0.5109	0.5461	0.54588	0.555683
12		0.0245	0.0243	0.0246	0.0138	0.02395	0.02393	0.0272414
160	**1**	5.6485e004	5.6498e004	5.6498e004	5.6497	56498.3	56444.0	56498.7
80		7.0613e003	7.0629e003	7.0629e004	7.0621	7062.93	7056.3	7063.14
40		882.9863	883.1807	883.1890	882.7586	883.188	883.188	883.297
12		23.9581	23.9611	23.9636	23.8345	23.9630	23.9630	23.9959

*Shear correction factor is: $k_s = \frac{10(1+\upsilon)}{12+11\upsilon}$.

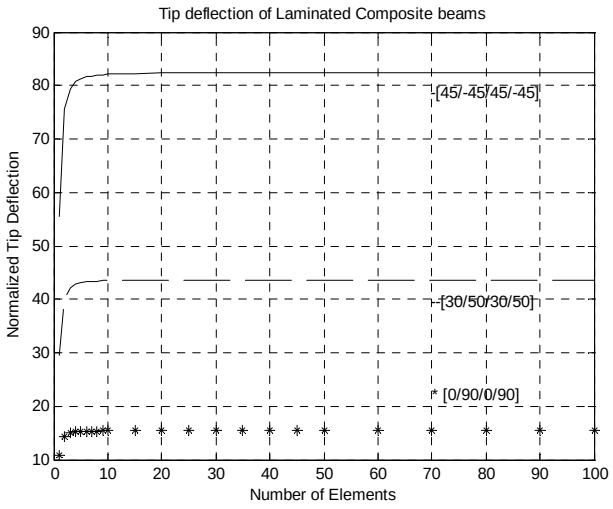

Figure 5. Normalized transverse tip deflections vs. number of elements of cantilever composite beams.

tip deflection of beams which is given as:
$\bar{W} = wAE_2h^2 10^2 / f_t L^4$, where w is the actual transversal deflection. It can be seen that the model predicttions are start to converge at reasonable number of elements for the different beams with different orientation angles.

In case of free vibration, the convergences of the natural frequencies of orthotropic beams with the same properties given above in this section are checked for two cases. The dimensionless frequency $\bar{\omega}$ is defined as:

$$\bar{\omega}_i = \omega_i L^2 \sqrt{\frac{\rho}{EIh^2}}$$

1) First case: Clamped-free beam with different orienttation angles [45/-45/45/-45], [30/50/30/50], and [0/90/0/90]. The obtained results of the dimensionless first natural frequency are shown in **Figure 6** for different number of elements.

2) Second Case: Clamped-free and clamped-clamped composite beams with stacking sequences [45/-45/45/-45], with number of elements changed from 10 to 40. The obtained results are presented in **Tables 8** and **9**.

It is clear from **Figure 6**, **Tables 8** and **9** that as the number of elements increases the natural frequency decreases until it reaches a constant value.

b) Static Validation

To check the validity of the model for orthotropic beam, two layer [0/90], three layer [0/90/0], four layer [0/90/0/90] and 10-layer [0/90/0/90..] lay-up are considered with material properties given above (case II:

Copyright © 2013 SciRes.

Table 5. (a) Non-dimensional frequency $\bar{\omega}$ of clamped-clamped aluminum beam (Modes: 1 - 5); (b) Non-dimensional frequency $\bar{\omega}$ of clamped-clamped aluminum beam (Modes: 6 - 10).

(a)

Method	*h*/*L*	$\bar{\omega}_1$	$\bar{\omega}_2$	$\bar{\omega}_3$	$\bar{\omega}_4$	$\bar{\omega}_5$
Present Model		4.7340	7.8675	11.0301	14.2049	17.3960
CBT		4.7300	7.8532	10.9956	14.1372	17.2788
FSDT	0.002	4.7299	7.8529	10.9949	14.1358	17.2765
TSDT		4.7299	7.8529	10.9949	14.1359	17.2766
CPM		4.7299	7.8529	10.9955	14.1359	17.2766
Present Model		4.7336	7.8662	11.0268	14.1982	17.3842
FSDT	0.005	4.7296	7.8516	10.9916	14.1293	17.2650
TSDT		4.7296	7.8516	10.9917	14.1294	17.2652
CPM		4.7296	7.8516	10.9917	14.1294	17.2651
Present Model		4.7324	7.8615	11.0150	14.1745	17.3424
FSDT	0.01	4.7283	7.8468	10.9799	14.1061	17.2244
TSDT		4.7284	7.8569	10.9801	14.1064	17.2249
CPM		4.7284	7.8469	10.9800	14.1062	17.2246
Present Model		4.7275	7.8426	10.9684	14.0818	17.1811
FSDT	0.02	4.7234	7.8281	10.9339	14.0154	17.0675
TSDT		4.7235	7.8283	10.9345	14.0167	17.0696
CPM		4.7235	7.8281	10.9341	14.0154	17.0679
Present Model		4.6937	7.7169	10.6705	13.5167	14.7532
FSDT	0.05	4.6898	7.7035	10.6399	13.4611	16.1586
TSDT		4.6902	7.7052	10.6447	13..4703	16.1754
CPM		4.6899	7.7035	10.6401	13.4611	16.1590
Present Model		4.5830	7.3419	9.8776	10.4321	12.1804
FSDT	0.1	4.5795	7.3312	9.8559	12.1453	14.2323
TSDT		4.5820	7.3407	9.8810	12.1861	14.3018

(b)

Method	*h*/*L*	$\bar{\omega}_6$	$\bar{\omega}_7$	$\bar{\omega}_8$	$\bar{\omega}_9$	$\bar{\omega}_{10}$
Present Model		20.6067	23.8404	27.1006	30.3908	33.7147
CBT		20.4204				
FSDT	0.002	20.4166				
TSDT		20.4170				
CPM		20.4168	23.5567	26.6960	29.8348	32.9729
Present Model		20.5876	23.8115	27.0587	30.3324	33.6356
FSDT	0.005	20.3983				
TSDT		20.3989				
CPM		20.3985	23.5292	26.6567	29.7808	32.9009
Present Model		20.5203	23.7098	26.9122	30.1291	32.9891
FSDT	0.01	20.3336				
TSDT		20.3350				
CPM		20.3338	23.4325	26.5192	29.5926	32.6514

Copyright © 2013 SciRes.

Continued

Present Model	0.02	20.2636	23.3268	23.3271	26.3697	29.3897
FSDT		20.0866				
TSDT		20.0911				
CPM		20.0868	23.0682	26.0086	28.9052	31.7558
Present Model	0.05	16.2480	18.8621	20.8641	21.3612	23.7503
FSDT		18.7316				
TSDT		18.7573				
CPM		18.7318	21.1825	23.5168	25.7421	27.8662
Present Model	0.1	14.2830	14.7532	16.2164	18.0075	18.0689
FSDT		16.1478				
TSDT		16.2373				
CPM		16.1487	17.9215	19.5723	21.1185	22.5735
Present Model	0.2	10.4321	11.3672	12.6631	12.7766	13.4580
FSDT		12.6357				
TSDT		12.8563				
CPM		12.6402	13.4567	13.8101	14.4806	14.9383

Table 6. (a) Non-dimensional frequency $\bar{\omega}$ of Free-Free aluminum beam (Modes: 1 - 5); (b) Non-dimensional frequency $\bar{\omega}$ of Free-Free aluminum beam (Modes: 6 - 10).

(a)

Method	*h*/*L*	$\bar{\omega}_1$	$\bar{\omega}_2$	$\bar{\omega}_3$	$\bar{\omega}_4$	$\bar{\omega}_5$
Present Model	0.002	4.7340	7.8675	11.0301	14.2049	17.3960
CBT		4.7300	7.8532	10.9956	14.1372	17.2788
CPM		4.7300	7.8530	10.9952	14.1362	17.2770
Present Model	0.005	4.7336	7.8662	11.0268	14.1982	17.3842
CPM		4.7298	7.8521	10.9928	14.1311	17.2678
Present Model	0.01	4.7324	7.8615	11.0150	14.1745	17.3424
CPM		4.7292	7.8490	10.9843	14.1311	17.2350
Present Model	0.02	4.7275	7.8426	10.9684	14.0818	17.1811
CPM		4.7265	7.8367	10.9508	14.0426	17.1078
Present Model	0.05	4.6937	7.7169	10.6705	13.5167	14.7532
CPM		4.7087	7.7540	10.7332	13.6040	16.3550
Present Model	0.1	4.5830	7.3419	9.8776	10.4321	12.1804
CPM		4.6484	7.4971	10.1255	12.5076	14.6682
Present Model	0.2	4.2444	6.4238	7.3766	8.2949	9.9175
CPM		4.44958	6.80257	8.7728	10.4094	11.7942

(b)

Method	*h*/*L*	$\bar{\omega}_6$	$\bar{\omega}_7$	$\bar{\omega}_8$	$\bar{\omega}_9$	$\bar{\omega}_{10}$
Present Model	0.002	20.6067	23.8404	27.1006	30.3908	33.7147
CBT		20.4204	23.5619	26.7035	29.8451	32.9869
CPM		20.4168	23.5567	26.6960	29.8348	32.9729
Present Model	0.005	20.5876	23.8115	27.0587	30.3324	33.6356
CPM		20.3985	23.5292	26.6567	29.7808	32.9009
Present Model	0.01	20.5203	23.7098	26.9122	30.1291	32.9891
CPM		20.3338	23.4325	26.5192	29.5926	32.6514
Present Model	0.02	20.2636	23.3268	23.3271	26.3697	29.3897
CPM		20.0868	23.0682	26.0086	28.9052	31.7558
Present Model	0.05	16.2480	18.8621	20.8641	21.3612	23.7503
CPM		18.7318	21.1825	23.5168	25.7421	27.8662
Present Model	0.1	14.2830	14.7532	16.2164	18.0075	18.0689
CPM		16.1487	17.9215	19.5723	21.1185	22.5735
Present Model	0.2	10.4321	11.3672	12.6631	12.7766	13.4580
CPM		12.6402	13.4567	13.8101	14.4806	14.9383

Copyright © 2013 SciRes.

Table 7. (a) Non-dimensional frequency $\bar{\omega}$ of simply supported aluminum beam (Modes: 1 - 5); (b) Non-dimensional frequency $\bar{\omega}$ of simply supported aluminum beam (Modes: 6 - 10).

(a)

Method	*h/L*	$\bar{\omega}_1$	$\bar{\omega}_2$	$\bar{\omega}_3$	$\bar{\omega}_4$	$\bar{\omega}_5$
Present Model		3.9682	6.2870	9.8995	12.5967	16.0886
CBT		3.1415	6.2831	9.4247	12.5664	15.7080
FSDT	0.002	3.1415	6.2831	9.4244	12.5656	15.7066
TSDT		3.1415	6.2831	9.4244	12.5656	15.7066
CPM		3.1415	6.2831	9.42449	12.5657	15.7066
Present Model		3.9680	6.2859	9.8972	12.5878	16.0785
FSDT	0.005	3.1415	6.2826	9.4229	12.5621	15.6996
TSDT		3.1415	6.2826	9.4229	12.5621	15.6996
CPM		3.1458	6.2826	9.4229	12.5621	15.6997
Present Model		3.9675	6.2820	9.8890	12.5560	16.0428
FSDT	0.01	3.1413	6.2810	9.4176	12.5494	15.6749
TSDT		3.1413	6.2810	9.4176	12.5494	15.6749
CPM		3.1413	6.28106	9.4176	12.5494	15.6749
Present Model		3.9651	6.2665	9.8568	12.4255	15.9031
FSDT	0.02	3.1405	6.2747	9.3962	12.4993	15.5784
TSDT		3.1405	6.2747	9.3963	12.4994	15.5784
CPM		3.1405	6.2747	9.3963	12.4994	15.5784
Present Model		3.9492	6.1615	9.6476	11.3774	14.0499
FSDT	0.05	3.1349	6.2313	9.2553	12.1812	14.9926
TSDT		3.1349	6.2313	9.2554	12.1816	14.9935
CPM		3.1349	6.2313	9.2553	12.1813	14.9926
Present Model		3.8954	5.8274	8.7928	9.0629	11.9071
FSDT	0.1	3.1156	6.0906	8.8404	11.3430	13.6131
TSDT		3.1156	6.0908	8.8414	11.3463	13.6207
CPM		3.1156	6.0906	8.8405	11.3431	13.6132
Present Model		3.7163	4.9163	6.7096	7.7592	8.9972
FSDT	0.2	3.0453	5.6715	7.8394	9..6569	11.2219
TSDT		3.0454	5.6731	7.8469	9..6769	11.2625
CPM		3.0453	5.6715	7.8395	9.6570	11.2220

(b)

Method	*h/L*	$\bar{\omega}_6$	$\bar{\omega}_7$	$\bar{\omega}_8$	$\bar{\omega}_9$	$\bar{\omega}_{10}$
Present Model		18.9519	22.4051	25.3759	28.8340	31.8919
CBT		18.8496				
FSDT	0.002	18.8471				
TSDT		18.8472				
CPM		18.8473	21.9875	25.1273	28.2666	31.4053
Present Model		18.9210	22.3771	25.2969	28.7725	31.7125
FSDT	0.005	18.8351				
TSDT		18.8352				
CPM		18.8352	21.9684	25.0988	28.2261	31.3498
Present Model		18.8040	22.2776	24.9347	28.5501	30.1074
FSDT	0.01	18.7925				
TSDT		18.7926				
CPM		18.7926	21.9011	24.9988	28.0845	31.1568
Present Model	0.02	18.1912	21.8533	25.6010	27.5289	31.0944
FSDT		18.6280				

Copyright © 2013 SciRes.

Continued

TSDT		18.6283				
CPM		18.6282	21.6443	24.6227	27.5599	30.4533
Present Model		15.0310	18.1814	18.7506	21.2668	22.4366
FSDT	0.05	17.6802				
TSDT		17.6829				
CPM		17.6810	20.2447	22.6862	25.0111	27.2263
Present Model		12.5912	14.4335	15.4982	16.8029	17.7914
FSDT	0.1	15.6769				
TSDT		15.6938				
CPM		15.6790	17.5705	19.3142	20.9325	22.4441
Present Model		9.8280	11.0553	11.4174	12.7520	12.9442
FSDT	0.2	12.5971				
TSDT		12.6723				
CPM		12.6022	13.0323	13.4443	13.8433	14.4378

Table 8. Convergence Test of the Non-dimensional frequency $\bar{\omega}$ of clamped-free composite beam [45/-45/45/-45] for different number of elements.

Mode	NE = 10	NE = 15	NE = 20	NE = 25	NE = 30	NE = 35	NE = 40
1	0.2720	0.2717	0.2716	0.2716	0.2715	0.2715	0.2715
2	1.5491	1.5394	1.5361	1.5345	1.5337	1.5331	1.5328
3	3.8246	3.7821	3.7673	3.7604	3.7567	3.7544	3.7530
4	4.3568	4.3472	4.3441	4.3427	4.3419	4.3415	4.3412
5	6.8480	6.7114	6.6646	6.6432	6.6316	6.6246	6.6201
6	9.7855	9.5498	9.4668	9.4283	9.4074	9.3948	9.3867
7	11.9164	11.8383	11.8098	11.7961	11.7884	11.7837	11.7807
8	13.4154	12.9864	12.8371	12.7686	12.7315	12.7093	12.6949
9	16.9935	16.4852	16.2544	16.1445	16.0843	16.0479	16.0242
10	17.3572	17.0537	16.9822	16.9491	16.9308	16.9196	16.9123
11	21.2396	20.3714	20.0318	19.8733	19.7871	19.7352	19.7015
12	21.5198	21.1988	21.0674	20.9990	20.9594	20.9345	20.9180
13	25.4546	24.3363	23.8845	23.6753	23.5625	23.4949	23.4512
14	25.5765	25.1350	24.9122	24.7934	24.7237	24.6797	24.6504
15	29.1905	28.3194	27.7288	27.4553	27.3083	27.2205	27.1640
16	29.7930	29.0617	28.7242	28.5422	28.4350	28.3672	28.3218
17	33.0389	32.3121	31.5622	31.2100	31.0205	30.9074	30.8345
18	35.0675	33.0663	32.5801	32.3165	32.1612	32.0628	31.9969
19	38.3174	36.0922	35.2609	34.8451	34.6177	34.4811	34.3928
20	39.4415	37.1951	36.5094	36.1401	35.9230	35.7857	35.6938
21	40.5941	38.6790	38.2294	37.9383	37.7590	37.6444	37.5676
22	43.6655	40.9089	40.1104	39.7272	39.5226	39.3901	39.2937
23	45.9351	41.4887	40.5512	40.0367	39.7497	39.5847	39.4873
24	46.7479	44.4977	43.5452	42.9445	42.6051	42.3981	42.2631
25	48.8336	45.6517	44.6932	43.9949	43.5922	43.3418	43.1761

Copyright © 2013 SciRes.

Table 9. Convergence Test of the Non-dimensional frequency $\bar{\omega}$ of clamped-clamped composite beam [45/-45/45/-45] for different number of elements.

Mode	NE = 10	NE = 15	NE = 20	NE = 25	NE = 30	NE = 35	NE = 40
1	1.5729	1.5583	1.5533	1.5509	1.5497	1.5489	1.5484
2	3.8328	3.7683	3.7463	3.7362	3.7308	3.7275	3.7253
3	6.6584	6.5004	6.4466	6.4220	6.4087	6.4007	6.3955
4	8.0017	7.9948	7.9918	7.9903	7.9894	7.9889	7.9886
5	9.8815	9.5910	9.4920	9.4466	9.4222	9.4075	9.3979
6	12.8693	12.5052	12.3672	12.3020	12.2664	12.2448	12.2307
7	14.4732	14.3429	14.3069	14.2915	14.2835	14.2787	14.2756
8	16.4714	15.8920	15.6705	15.5659	15.5085	15.4738	15.4512
9	19.1131	18.9127	18.8466	18.8159	18.7991	18.7889	18.7823
10	20.2369	19.4491	19.1301	18.9778	18.8941	18.8433	18.8102
11	23.3548	22.9878	22.7437	22.5351	22.4201	22.3502	22.3047
12	24.1391	23.1764	22.8551	22.7910	22.7550	22.7329	22.7184
13	27.5397	26.9554	26.4557	26.1808	26.0290	25.9368	25.8768
14	27.9391	27.0202	26.7222	26.6072	26.5422	26.5019	26.4753
15	30.4178	30.9370	30.2242	29.8713	29.6760	29.5574	29.4801
16	32.3233	30.9640	30.5898	30.4038	30.2981	30.2325	30.1890
17	36.5307	34.9088	34.0405	33.5978	33.3517	33.2020	33.1045
18	38.9175	35.0795	34.5157	34.2330	34.0723	33.9725	33.9064
19	41.3899	38.8894	37.8856	37.3452	37.0424	36.8576	36.7371
20	42.6706	39.3305	38.5317	38.1201	37.8867	37.7421	37.6464
21	44.4803	41.4014	41.3918	41.1277	40.7610	40.5364	40.3896
22	46.3000	42.8597	41.7755	41.3862	41.3801	41.3692	41.3413
23	50.0105	43.6673	42.6605	42.0841	41.7603	41.5674	41.4607
24	52.1104	46.6610	45.7004	44.9406	44.5058	44.2382	44.0628
25	55.4025	47.3440	46.9088	46.1264	45.6792	45.4038	45.2225

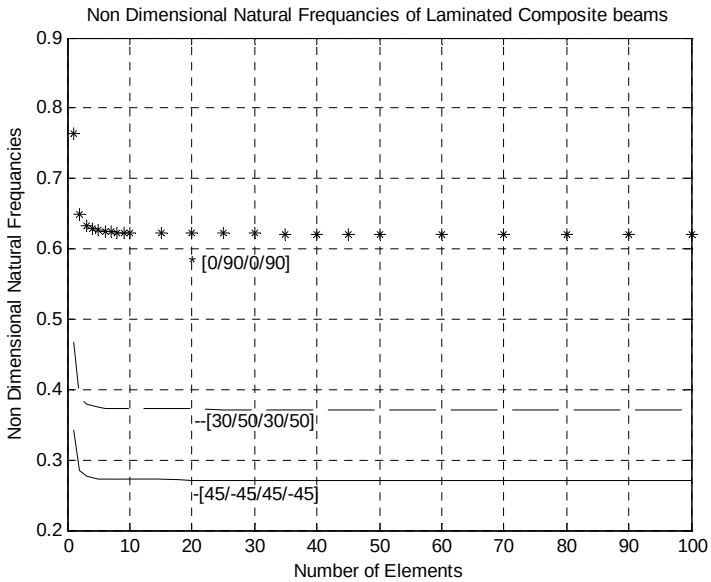

Figure 6. Non-dimensional first natural frequency vs. number of elements of cantilever composite beams.

Copyright © 2013 SciRes.

orthotropic beam). Different length to height ratio L/h = 5, 10, and 50 are used to validate the proposed model. All laminas are assumed to be of the same thickness and made of the same materials. The number of elements is taken equal to 33. The mid span deflection is chosen in the validation in order to compare the obtained results with different theories reported in [12] and [14]. These predictions are given in **Tables 10-12**.

Table 10. (a) Non-dimensional mid-span deflection of symmetric cross-ply beams [0/90/0] for various boundary conditions; (b) Non-dimensional mid-span deflection of anti-symmetric cross-ply beams [0/90] for various boundary conditions.

(a)

L/h	Theory	S-S	C-S	C-C	C-F
5	**Present Model**	2.4240	2.1814	1.8540	6.2792
	HOBT*	2.412	1.952	1.537	6.824
	SOBT*	1.896	1.655	1.379	5.948
	FOBT*	2.146	1.922	1.629	6.698
	RFSDT**	2.145	1.921	1.629	6.693
	CBT*	0.646	0.259	0.129	2.198
10	**Present Model**	1.1383	0.7825	0.5694	2.4221
	HOBT	1.096	0.740	0.532	3.455
	SOBT	0.959	0.622	0.442	3.135
	FOBT	1.021	0.693	0.504	3.323
	RFSDT	1.020	0.693	0.504	3.321
	CBT	0.646	0.259	0.129	2.198
50	**Present Model**	0.7268	0.3077	0.1584	1.1878
	HOBT	0.665	0.280	0.147	2.251
	SOBT	0.659	0.273	0.142	2.235
	FOBT	0.661	0.276	0.144	2.243
	RFSDT	0.660	0.276	0.144	2.242
	CBT	0.646	0.259	0.129	2.198

*Reference [12]. **Reference [14].

(b)

L/h	Theory	S-S	C-S	C-C	C-F
5	**Present Model**	5.0418	3.3341	2.3750	17.1281
	HOBT*	4.777	2.863	1.922	15.279
	SOBT*	4.800	3.035	2.124	15.695
	FOBT*	5.036	3.320	2.379	16.436
	RFSDT**	5.048	3.324	2.381	16.496
	CBT*	3.322	1.329	0.664	11.293
10	**Present Model**	3.7560	1.8520	1.0905	13.1942
	HOBT	3.688	1.740	1.005	12.343
	SOBT	3.692	1.764	1.032	12.400
	FOBT	3.750	1.834	1.093	12.579
	RFSDT	3.751	1.835	1.094	12.607
	CBT	3.322	1.329	0.664	11.293
50	**Present Model**	3.3446	1.3677	0.6794	11.9354
	HOBT	3.336	1.346	0.679	11.337
	SOBT	3.336	1.346	0.679	11.338
	FOBT	3.339	1.349	0.681	11.345
	RFSDT	3.353	1.356	0.686	11.413
	CBT	3.322	1.329	0.664	11.293

*Reference [12]. **Reference [14].

Copyright © 2013 SciRes.

Table 11. Comparison of natural frequencies (kHz) of simply supported $\left[0^0\right]$ composite beams.

L/h		Frequency (kHz)			
	Mode	**Present Model**	**FSDT [30]**	**CLT [14]**	**RFSDT [14]**
120	**1**	0.0506	0.051	0.051	0.051
	2	0.2018	0.203	0.203	0.202
	3	0.4519	0.457	0.457	0.453
	4	0.7982	0.812	0.812	0.802
	5	1.2373	1.269	1.269	1.248
15	**1**	0.7504	0.755	0.813	0.755
	2	2.5244	2.548	3.250	2.563
	3	4.6758	4.716	7.314	4.816
	4	6.9148	6.960	13.00	7.283
	5	9.1529	9.194	20.32	9.935

Table 12. Comparison of non-dimensional natural frequencies of symmetrically laminated cross-ply and angle-ply beams under various boundary conditions.

	[0/90/90/0]				**[45/-45/-45/45]**			
Boundary Condition	**Present Model**	**FSDT Exact [2-30]**	**RFSDT [14]**	**HSDT [2]**	**Present Model**	**FSDT Exact [2-30]**	**RFSDT [14]**	**HSDT [2]**
S-S	2.4864	2.4978	2.507	2.5023	0.9033	1.5368	1.526	0.8295
C-C	4.5817	4.6602	4.606	4.5940	1.9823	3.1843	3.170	1.8472
C-S	3.5084	3.5446	3.533	3.5254	1.3902	2.3032	2.289	1.2855
C-F	0.9196	0.9231	0.925	0.9241	0.3244	0.5551	0.551	0.2965

It is shown in **Table 10(a)** that the non-dimensional mid-span deflections of symmetric cross-ply beams are better than CBT, FSDT and HSDT theories for all L/h ratios, however for C-F case it is better than CBT only and poor than FSDT and HSDT theories, known that the a few seconds are taken to complete the single run of the code.

It is shown in **Table 10(b)** that the non-dimensional mid-span deflections of symmetric cross-ply beams are better than all theories for all values of *L*/*h* ratios, for the various proposed boundary conditions. Large differences between the results of the refined theories and the classical theory are noted, especially when the *L*/*h* ratio decreases (*L*/*h* less than or equal to 5), indicating the effect of shear deformation. It is seen that the symmetric cross-ply stacking sequence gives a smaller response than those of anti symmetric ones. The obtained results by the present model are close to the predictions of FOBT theory and the RFSDT reported in [12] and [14].

c) Dynamic Validation

To check the free vibration validity of the present model, An AS/3501-6 graphite/epoxy composite used in the analysis with the following properties:

$E_1 = 144.80$ GPa , $E_2 = 9.65$ GPa , $G_{23} = 3.34$ GPa , $G_{13} = G_{12} = 4.14$ GPa , $v_{12} = 0.3$, and $\rho = 1389.23\ \mathrm{Kg/m^3}$. The beam length to height ratio is $L/h = 15$. The non-dimensional fundamental natural frequency is given by: $\bar{\omega} = \omega L^2 \sqrt{\left(\rho / E_1 h^2\right)}$, where ω and ρ are the free natural frequency and mass of the material of the beam, respectively. All laminas are assumed to be of the same thickness and made of the same materials. The obtained results are given in **Tables 11-13**, and they compared with different theories reported in [2], [14], and [30].

Table 11 shows the comparisons of the first five natural frequencies of a long thin (*L*/*h* = 120) and a short thick (*L*/*h* = 15) simply supported unidirectional $\left(0^0\right)$ composite beam. It seen that the proposed element prediction are better than the results obtained from the RFSDT [14], which used the same assumed displacement equations as the present model, but its element has two nodes with total six degrees of freedom. Also the present model predictions are in good agreement with the available results for both thin and thick beams.

Table 12 shows the comparison of the non-dimensional natural frequencies of symmetrically laminated cross-ply [0/90/0/90] and angle-ply [45/-45/45/-45] beams for various boundaries. For cross-ply the obtained results

Copyright © 2013 SciRes.

are much closed to the results obtained by other methods (exact FSDT, RFSDT, and HSDT). For angle-ply the obtained results are much closer to the results of [6] using HSDT with FE, and deviate from the results of the exact solution [30] which reported in [2], and the results obtained from RFSDT [14].

Table 13 shows the first five natural frequencies for different un-symmetrically lamination in comparison with [2], good agreement is found.

The effect of the boundary conditions on the first five natural frequencies of anti-symmetric angle ply beams is shown in **Table 14**. The obtained results from the present model for different boundary conditions are much closed to the results of [2], which used HSDT.

8. Conclusions

The following conclusions have been drawn:

1) Finite element model has been obtained for static deformation and free vibration analysis of isotropic and orthotropic beams based on first order shear deformation theory, Timoshenko beam theory.

2) Various results have been presented to show the effect of number of elements, boundary conditions, length to thickness ratio L/h, material properties, number of layers, and ply orientation, on the static deflection and natural frequency of the proposed models.

3) The proposed model is valid to decrease the error due to un-accurately modeling of the curvature present in the actual material under bending which known as shear Locking.

4) The code running time is around few second for both deflection and natural frequency calculation using number of elements equal 33 on PC Pentium 3.

5) The model results are converging at small number of elements for deflection and natural frequency for isotropic and orthotropic beams.

6) In case isotropic beam subjected to uniform distributed loads the static analysis shows that for length to thickness ratio L/h less than 20 the proposed model gives more accurate results than the exact formula of Timoshenko and Euler beams. For L/h greater than 20 the obtained results values are start to be less than Timoshenko based solution and get gradually closer to Euler solution.

7) Also for isotropic beam subjected to concentrated tip load the model accuracy is in between the HSDT, the finite element and other different solutions. Also the shear correction factor affects the obtained results.

Table 13. Effect of ply orientation angles on the non-dimensional natural frequencies of un-symmetric clamped-clamped beams.

Mode	[0/90/0/90]		[45/-45/45/-45]		[30/50/30/50]	
	Present Model	Ref. [2]	Present Model	Ref. [2]	Present Model	Ref. [2]
1	3.6892	3.7244	1.9823	1.9807	2.5785	2.2526
2	8.7141	8.9275	5.1365	5.2165	6.4915	5.8624
3	14.7975	15.3408	9.3709	9.6912	11.5440	10.7609
4	21.3950	22.3940	14.2009	10.5345	17.2278	11.9506
5	28.3580	24.3155	14.9973	15.0981	19.9716	16.5747

Table 14. Effect of boundary conditions on the non-dimensional natural frequencies of anti-symmetric laminated angle ply beams [45/-45/45/-45].

Method	Beam Type	Mode number				
		1	2	3	4	5
Present Model	C-F	0.3244	1.9497	5.1413	7.5737	9.5140
Ref. [2]		0.2962	1.8156	4.9163	5.3660	9.2162
Present Model	S-S	0.9033	3.4642	7.3364	12.1458	14.8566
Ref. [2]		0.8278	3.2334	7.0148	10.7449	11.9145
Present Model	S-C	1.3902	4.2774	8.3468	13.2232	14.8797
Ref. [2]		1.2786	4.0139	8.0261	10.7449	13.0579
Present Model	S-F	1.3919	4.2810	7.4965	8.5410	13.3071
Ref. [2]		1.2883	4.0653	5.3660	8.1608	13.3136
Present Model	C-C	1.9823	5.1365	9.3709	14.2009	14.9973
Ref. [2]		1.8298	4.8472	9.0601	10.7449	14.1999

Copyright © 2013 SciRes.

8) In case isotropic beam, generally, for small value of L/h (h/L equal to or greater than 0.05), the model results are better than all other theories CBT, exact FSDT (EFSDT), CPT, and HSDT for various boundary conditions. However, for the ratio L/h greater than a value around 20, generally, the model results were closer to the results of other theories.

9) For cross-ply orthotropic composite beams the obtained deflections are better than all other theories for all values of L/h and for all boundary conditions, except (C-F) case, the EFSDT and HSDT were better. However, for angle-ply beams the proposed model is better than all.

10) For cross-ply and angle-ply orthotropic composite beam the natural frequency are accepted in compared with EFSDT and HSDT, and better than RFSDT.

11) The model gives natural frequency of composite beam better than EFSDT and HSDT for S-S, S-F, C-C boundary conditions, and it were closer to these theories for other C-F and S-S boundary conditions.

REFERENCES

[1] F. G. Yuan and R. E. Miller, "A New Finite Element for Laminated Composite Beams," *Computers and Structures*, Vol. 31, No. 5, 1989, pp. 737-745. doi:10.1016/0045-7949(89)90207-1

[2] K. Chandrashekhara and K. M. Bangera, "Free Vibration of Composite Beams Using a Refined Shear Flexible Beam Element," *Computers and Structures*, Vol. 43, No. 4, 1992, pp. 719-727. doi:10.1016/0045-7949(92)90514-Z

[3] Z. Friedman and J. B. Kosmatka, "An Improved Two-Node Timoshenko Beam Finite Element," *Computer and Structures*, Vol. 47, No. 3, 1993, pp. 473-481. doi:10.1016/0045-7949(93)90243-7

[4] T. Lidstrom, "An Analytical Energy Expression for Equilibrium Analysis of 3-D Timoshenko Beam Element," *Computers and Structures*, Vol. 52, No. 1, 1994, pp. 95-101. doi:10.1016/0045-7949(94)90259-3

[5] S. R. Bhate, U. N. Nayak and A. V. Patki, "Deformation of Composite Beam Using Refined Theory," *Computers and Structures*, Vol. 54, No. 3, 1995, pp. 541-546. doi:10.1016/0045-7949(94)00354-6

[6] S. M. Nabi and N. Ganesan, "Generalized Element for the Free Vibration Analysis of Composite Beams," *Computers and Structures*, Vol. 51, No. 5, 1994, pp. 607-610. doi:10.1016/0045-7949(94)90068-X

[7] E. A. Armanios and A. M. Badir, "Free Vibration Analysis of the Anisotropic Thin-Walled Closed-Section Beams," *Journal of the American Institute of Aeronautics and Astronautics*, Vol. 33, No. 10, 1995, pp. 1905-1910. doi:10.2514/3.12744

[8] V. Giavotto, M. Borri, P. Mantegazza, G. Ghiringhelli, V. Carmash, G. Maffioli and F. Mussi, "Anisotropic Beam Theory And Applications," *Computers and Structures*, Vol. 16, No. 4, 1983, pp. 403-413. doi:10.1016/0045-7949(83)90179-7

[9] D. Hagodes, A. Atilgan, M. Fulton and L. Rehfield, "Free Vibration Analysis of Composite Beams," *Journal of the American Helicopter Society*, Vol. 36, No. 3, 1991, pp. 36-47. doi:10.4050/JAHS.36.36

[10] R. Chandra and I. Chopra, "Experimental and Theoretical Investigation of the Vibration Characteristics of Rotating Composite Box Beams," *Journal of Aircraft*, Vol. 29, No. 4, 1992, pp. 657-664. doi:10.2514/3.46216

[11] S. R. Rao and N. Ganesan, "Dynamic Response of Tapered Composites Beams Using Higher Order Shear Deformation Theory," *Journal of Sound and Vibration*, Vol. 187, No. 5, 1995, pp. 737-756. doi:10.1006/jsvi.1995.0560

[12] A. A. Khdeir and J. N. Reddy, "An Exact Solution for the Bending of Thin and Thick Cross-Ply Laminated Beams," *Computers and Structures*, Vol. 37, 1997, pp. 195-203. doi:10.1016/S0263-8223(97)80012-8

[13] V. Yildirm, E. Sancaktar and E. Kiral, "Comparison of the In-Plan Natural Frequencies of Symmetric Cross-Ply Laminated Beams Based On The Bernoulli-Eurler and Timoshenko Beam Theories," *Journal of Applied Mechanics*, Vol. 66, No. 2, 1999, pp. 410-417. doi:10.1115/1.2791064

[14] A. Chakraborty, D. R. Mahapatra and S. Gopalakrishnan, "Finite Element Analysis of Free vibration and Wave Propagation in Asymmetric Composite Beams With Structural Discontinuities," *Composite Structures*, Vol. 55, No. 1, 2002, pp. 23-36. doi:10.1016/S0263-8223(01)00130-1

[15] M. Eisenberger, "An Exact High Order Beam Element," *Computer and Structures*, Vol. 81, No. 3, 2003, pp. 147-152. doi:10.1016/S0045-7949(02)00438-8

[16] J. Lee and W. W. Schultz, "Eigenvalue Analysis of Timoshenko Beams and Axi-symmetric Mindlin Plates by the Pseudospectral Method," *Journal of Sound and Vibration*, Vol. 269, No. 3-5, 2004, pp. 609-621. doi:10.1016/S0022-460X(03)00047-6

[17] P. Subramanian, "Dynamic Analysis of Laminated Composite Beams Using Higher Order Theories and Finite Elements," *Composite and Structures*, Vol. 73, No. 3, 2006, pp. 342-353. doi:10.1016/j.compstruct.2005.02.002

[18] M. Simsek and T. Kocaturk, "Free Vibration Analyses of Beams by Using a Third-Order Shear Deformation Theory," *Sadana*, Vol. 32, Part 3, 2007, pp. 167-179. doi:10.1007/s12046-007-0015-9

[19] L. Jun, H. Hongxinga and S. Rongyinga, "Dynamic Finite Element Method for Generally Laminated Composite Beams," *International Journal of Mechanical Sciences*, Vol. 50, No. 3, 2008, pp. 466-480. doi:10.1016/j.ijmecsci.2007.09.014

[20] U. Lee and I. Jang, "Spectral Element Model for Axially Loaded Bending-Shear-Torsion Coupled Composite Timoshenko Beams," *Composite Structures*, Vol. 92, No. 12, 2010, pp. 2860-2870. doi:10.1016/j.compstruct.2010.04.012

[21] Q. H. Nguyen, E. Martinellib and M. Hjiaja, "Derivation of the Exact Stiffness Matrix for a Two-Layer Timoshenko Beam Element with Partial Interaction," *Engineering Structures*, Vol. 33, No. 2, 2011, pp. 298-307. doi:10.1016/j.engstruct.2010.10.006

Copyright © 2013 SciRes.

[22] X. Lina and Y. X. Zhang, "A Novel One-Dimensional Two-Node Shear-Flexible Layered Composite Beam Element," *Finite Elements in Analysis and Design*, Vol. 47, No. 7, 2011, pp. 676-682. doi:10.1016/j.finel.2011.01.010

[23] G. J. Kennedya, J. S. Hansena and J. R. R. A Martinsb, "A Timoshenko Beam Theory with Pressure Corrections for Layered Orthotropic Beams," *International Journal of Solids and Structures*, Vol. 48, No. 16-17, 2011, pp. 2373-2382. doi:10.1016/j.ijsolstr.2011.04.009

[24] J. N. Reddy, "An Introduction to Nonlinear Finite Element Analysis," Oxford University Press, USA, 2004.

[25] J. N. Reddy, "Mechanics of Laminated Composite Plates and Shells-Theory and Analysis," 2nd Edition, CRC Press, USA, 2004.

[26] S. S. Rao, "The Finite Element Method in Engineering," 2nd Edition, BPCC Wheatons Ltd., Exeter, 1989, pp. 206-207.

[27] R. D. Cook, D. S. Malkus and M. E. Plesha, "Concept and Applications of Finite Element Analysis," 3rd Edition, John Wiley & Sons, 1974, p. 96.

[28] W. C. Hurty and M. F. Rubinstein, "Dynamics of Structures," Prentice Hall, New Delhi, 1967.

[29] T. Kocaturk and M. Simsek, "Free Vibration Analysis of Timoshenko Beams under Various Boundary Conditions," *Sigma Journal of Engineering and Natural Science*, Vol. 1, 2005, pp. 30-44.

[30] K. Chandrashekhara, K. Krishnamurthy and S. Roy, "Free Vibration of Composite Beams Using a Refined Shear Flexible Beam Element," *Computers and Structures*, Vol. 14, No. 4, 1990, pp. 269-279. doi:10.1016/0263-8223(90)90010-C

Copyright © 2013 SciRes.

Appendix A

The element mass matrix for the Timoshenko Beam:

$$\begin{bmatrix}
\frac{8}{105}mL & 0 & \frac{-13}{240}mhL & \frac{33}{560}mL & 0 & \frac{-3}{140}mL & \frac{19}{1680}mL & 0 & \frac{-1}{120}mhL \\
0 & \frac{2}{15}mL & 0 & 0 & \frac{1}{15}mL & 0 & 0 & \frac{-1}{30}mL & 0 \\
\frac{-13}{240}mhL & 0 & \frac{1}{9}mh^2L & \frac{-3}{20}mhL & 0 & \frac{-3}{80}mhL & \frac{-1}{120}mhL & 0 & \frac{1}{18}mh^2L \\
\frac{33}{560}mL & 0 & \frac{-3}{20}mhL & \frac{27}{70}mL & 0 & \frac{-27}{560}mL & \frac{-3}{140}mL & 0 & \frac{-3}{80}mhL \\
0 & \frac{1}{15}mL & 0 & 0 & \frac{8}{15}mL & 0 & 0 & \frac{1}{15}mL & 0 \\
\frac{-3}{140}mL & 0 & \frac{-3}{80}mhL & \frac{-27}{560}mL & 0 & \frac{27}{70}mL & \frac{33}{560}mL & 0 & \frac{-3}{20}mhL \\
\frac{19}{1680}mL & 0 & \frac{-1}{120}mhL & \frac{-3}{140}mL & 0 & \frac{33}{560}mL & \frac{8}{105}mL & 0 & \frac{-13}{240}mhL \\
0 & \frac{-1}{30}mL & 0 & 0 & \frac{1}{15}mL & 0 & 0 & \frac{2}{15}mL & 0 \\
\frac{-1}{120}mhL & 0 & \frac{1}{18}mh^2L & \frac{-3}{80}mhL & 0 & \frac{-3}{20}mhL & \frac{-13}{240}mhL & 0 & \frac{1}{9}mh^2L
\end{bmatrix} \quad \textbf{(A-1)}$$

where; $m = \rho bh$

The element stiffness matrix for orthotropic Timoshenko Beam:

$$\begin{bmatrix}
\frac{37A_{11}b}{10L} & 0 & \frac{-B_{11}b}{L} & \frac{-189A_{11}b}{40L} & 0 & \frac{27A_{11}b}{20L} & \frac{-13A_{11}b}{40L} & 0 & \frac{B_{11}b}{L} \\
0 & \frac{7k_sA_{55}b}{3L} & \frac{5k_sA_{55}b}{6} & 0 & \frac{-8k_sA_{55}b}{3L} & 0 & 0 & \frac{k_sA_{55}b}{3L} & \frac{k_sA_{55}b}{6} \\
\frac{-B_{11}b}{L} & \frac{5k_sA_{55}b}{6} & \frac{D_{11}b}{L}+\frac{k_sA_{55}Lb}{3} & 0 & \frac{-2k_sA_{55}b}{3} & 0 & \frac{B_{11}b}{L} & \frac{-k_sA_{55}b}{6} & \frac{-D_{11}b}{L}+\frac{k_sA_{55}Lb}{6} \\
\frac{-189A_{11}b}{40L} & 0 & 0 & \frac{54A_{11}b}{5L} & 0 & \frac{-297A_{11}b}{40L} & \frac{27A_{11}b}{20L} & 0 & 0 \\
0 & \frac{-8k_sA_{55}b}{3L} & \frac{-2k_sA_{55}b}{3} & 0 & \frac{16k_sA_{55}b}{3L} & 0 & 0 & \frac{-8k_sA_{55}b}{3L} & \frac{2k_sA_{55}b}{3} \\
\frac{27A_{11}b}{20L} & 0 & 0 & \frac{-297A_{11}b}{40L} & 0 & \frac{54A_{11}b}{5L} & \frac{-189A_{11}b}{40L} & 0 & 0 \\
\frac{-13A_{11}b}{40L} & 0 & \frac{B_{11}b}{L} & \frac{27A_{11}b}{20L} & 0 & \frac{-189A_{11}b}{40L} & \frac{37A_{11}b}{10L} & 0 & \frac{-B_{11}b}{L} \\
0 & \frac{k_sA_{55}b}{3L} & \frac{-k_sA_{55}b}{6} & 0 & \frac{-8k_sA_{55}b}{3L} & 0 & 0 & \frac{7k_sA_{55}b}{3L} & \frac{-5k_sA_{55}b}{6} \\
\frac{B_{11}b}{L} & \frac{k_sA_{55}b}{6} & \frac{-D_{11}b}{L}+\frac{k_sA_{55}Lb}{6} & 0 & \frac{2k_sA_{55}b}{3} & 0 & \frac{-B_{11}b}{L} & \frac{-5k_sA_{55}b}{6} & \frac{D_{11}b}{L}+\frac{k_sA_{55}Lb}{3}
\end{bmatrix} \quad \text{(A-2)}$$

The element load vector:

$$F = \begin{bmatrix} \frac{f_aL}{8} & P_1+\frac{f_tL}{6} & 0 & \frac{3f_aL}{8} & P_2+\frac{2f_tL}{3} & \frac{3f_aL}{8} & \frac{f_aL}{8} & P_3+\frac{f_tL}{6} & 0 \end{bmatrix}^t \quad \text{(A-3)}$$

Copyright © 2013 SciRes.

The element stiffness matrix for isotropic Timoshenko Beam is:

$$\begin{bmatrix}
\frac{37EA}{10L} & 0 & \frac{-EAh}{2L} & \frac{-189EA}{40L} & 0 & \frac{27EA}{20L} & \frac{-13EA}{40L} & 0 & \frac{EAh}{2L} \\
0 & \frac{7k_sGA}{3L} & \frac{5k_sGA}{6} & 0 & \frac{-8k_sGA}{3L} & 0 & 0 & \frac{k_sGA}{3L} & \frac{k_sGA}{6} \\
\frac{-EAh}{2L} & \frac{5k_sGA}{6} & \frac{EAh^2}{3L}+\frac{k_sGLA}{3} & 0 & \frac{-2k_sGA}{3} & 0 & \frac{EAh}{2L} & \frac{-k_sGA}{6} & \frac{-EAh^2}{3L}+\frac{k_sGLA}{6} \\
\frac{-189EA}{40L} & 0 & 0 & \frac{54ELA}{5} & 0 & \frac{-297EA}{40L} & \frac{27EA}{20L} & 0 & 0 \\
0 & \frac{-8k_sGA}{3L} & \frac{-2k_sGA}{3} & 0 & \frac{16k_sGA}{3L} & 0 & 0 & \frac{-8k_sGA}{3L} & \frac{2k_sGA}{3} \\
\frac{27EA}{20L} & 0 & 0 & \frac{-297EA}{40L} & 0 & \frac{54EA}{5L} & \frac{-189EA}{40L} & 0 & 0 \\
\frac{-13EA}{40L} & 0 & \frac{EAh}{2L} & \frac{27EA}{20L} & 0 & \frac{-189EA}{40L} & \frac{37EA}{10L} & 0 & \frac{-EAh}{2L} \\
0 & \frac{k_sGA}{3L} & \frac{-k_sGA}{6} & 0 & \frac{-8k_sGA}{3L} & 0 & 0 & \frac{7k_sGA}{3L} & \frac{-5k_sGA}{6} \\
\frac{EAh}{2L} & \frac{k_sGA}{6} & \frac{-EAh^2}{3L}+\frac{k_sGLA}{6} & 0 & \frac{2k_sGA}{3} & 0 & \frac{-EAh}{2L} & \frac{-5k_sGA}{6} & \frac{EAh^2}{3L}+\frac{k_sGLA}{3}
\end{bmatrix} \quad \text{(A-4)}$$

where; $A = bh$

Copyright © 2013 SciRes.

Nomenclature

Symbol	Definition
A	Beam cross section area.
A_{ij}	Elements of extensional stiffness matrix.
B_{ij}	Elements of coupling stiffness matrix.
b	Width of beam.
C_{ijkl}	Elastic constants.
c_1 , c_2 , c_3 and c_4	Constant coefficients.
D_{ij}	Elements of bending stiffness matrix.
E	Young's modulus.
E_1	Young's modulus in the fiber direction.
E_2	Young's modulus in the transversal direction to the fiber.
f_a , f_t	Axial and transversal forces.
G	Shear modulus.
h	Thickness of beam.
$[K]$	Element stiffness matrix.
k	Layer number in the laminated beam.
L	Length of beam.
$[M]$	Element mass matrix.
m	Mass per unit length of the beam.
N	Total number of layers of the laminated beam.
NE	Number of elements.
Q_{ij}	Components of the lamina stiffness matrix.
q and $\ddot{q}$	Generalized nodal displacements and its second derivative.
T	Kinetic energy.
U	Internal strain energy for the structure.
u, v, w	Displacements of any point in the x-, y-, and z directions.
u_1, u_2, u_3 and u_4	Axial displacements at the boundaries of beam element.
u° , v° , w°	Reference surface displacements along x-, y-, and z- axes.
W	Work done due to external loads.
$w_1, w_2,$ and w_3	Transversal displacements at the boundaries of beam element.
γ°_{xy}	Reference surface Transversal shear strain in x-z plane.
γ_{xz}	Transversal shear strain in x-z plane.
ε_x , ε_y , ε_z	Linear strains in the x-,y-, and x-directions.
ε°_x , ε°_y	Reference surface extension strains in x-, & y- directions.
ζ_i	Transversal displacement shape functions.
κ°_x , κ°_y	Reference surface curvatures in the x-, and y-directions.
ξ_i	Axial displacement shape functions.
ρ	Mass of the structure material.
σ_x	Normal stress in the x-direction.
σ_{xz}	Shear stress in the x-z plane.

Copyright © 2013 SciRes.

ω	Natural frequency of the structure.
ϕ_x	Angle of rotation.
ϕ_1 and ϕ_2	Rotation angles at nodes.
ς_1 and ς_2	Electrical potential shape functions.
ψ_i	Rotation displacement shape functions.
HSDT	Third-order shear deformation theory.
SSDT	Second-order shear deformation theory.
FSDT	First-order shear deformation theory.
RFSDT	Refined first-order shear deformation theory.
CBT	Classical beam theory.

Copyright © 2013 SciRes.